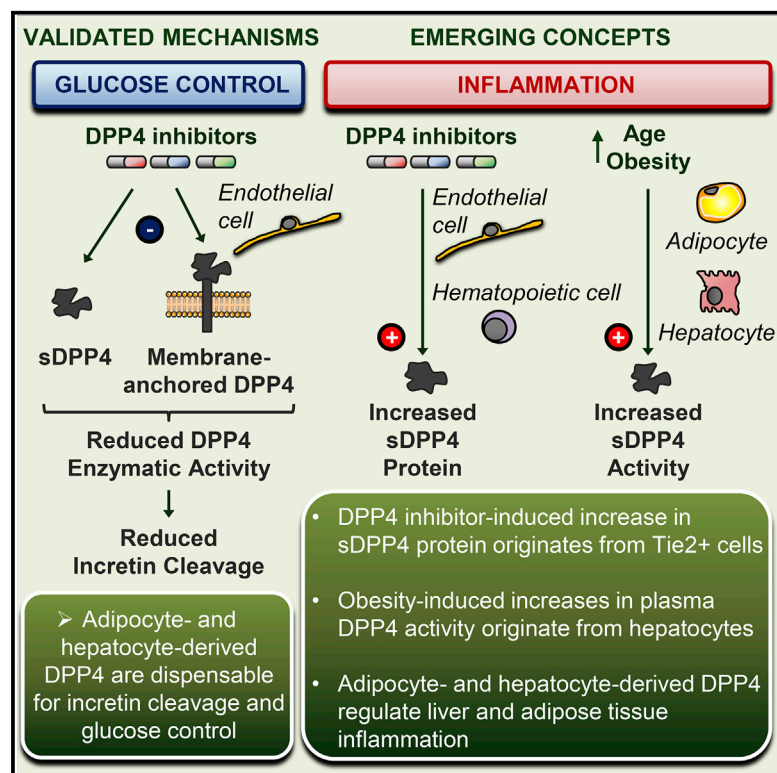


Cell Metabolism

Circulating Levels of Soluble Dipeptidyl Peptidase-4 Are Dissociated from Inflammation and Induced by Enzymatic DPP4 Inhibition

Graphical Abstract



Authors

Elodie M. Varin, Erin E. Mulvihill, Jacqueline L. Beaudry, ..., Dianne Matthews, Jonathan E. Campbell, Daniel J. Drucker

Correspondence

drucker@lunenfeld.ca

In Brief

Varin et al. report that DPP4 activity and sDPP4 protein differentially regulate glucose homeostasis and inflammation, and that this regulation is dependent upon the cellular source of DPP4. Remarkably, DPP4 inhibitors robustly induce plasma levels of sDPP4, revealing divergence of glucoregulatory DPP4 enzymatic activity versus levels of immuno-modulatory sDPP4.

Highlights

- Adipocyte DPP4 contributes to circulating sDPP4, but not to glucose homeostasis
- Hepatocyte DPP4 contributes to its circulating activity and hepatic/adipose inflammation
- Circulating, soluble DPP4 is markedly induced by systemic DPP4 enzymatic inhibition
- DPP4 activity and sDPP4 levels do not correlate with extent of metabolic inflammation



Circulating Levels of Soluble Dipeptidyl Peptidase-4 Are Dissociated from Inflammation and Induced by Enzymatic DPP4 Inhibition

Elodie M. Varin,^{1,4} Erin E. Mulvihill,^{1,4,5} Jacqueline L. Beaudry,¹ Gemma Pujadas,¹ Shai Fuchs,¹ Jean-François Tanti,² Sofia Fazio,² Kirandeep Kaur,¹ Xiemin Cao,¹ Laurie L. Baggio,¹ Dianne Matthews,¹ Jonathan E. Campbell,^{1,6} and Daniel J. Drucker^{1,3,7,*}

¹Lunenfeld-Tanenbaum Research Institute, Mt. Sinai Hospital, LTRI, 600 University Avenue TCP5-1004, Toronto, ON M5G 1X5, Canada

²INSERM U1065, Mediterranean Center of Molecular Medicine, University Côte d'Azur, Faculty of Medicine, 06204 Nice, France

³Department of Medicine, University of Toronto, Toronto, ON M5S 2J7, Canada

⁴These authors contributed equally

⁵Present address: University of Ottawa Heart Institute, 40 Ruskin Street, Ottawa, ON H-3228A, Canada

⁶Present address: Duke Molecular Physiology Institute, 49-102, 300 N. Duke St. Durham, NC 27701, USA

⁷Lead Contact

*Correspondence: drucker@lunenfeld.ca

<https://doi.org/10.1016/j.cmet.2018.10.001>

SUMMARY

Dipeptidyl peptidase-4 (DPP-4) controls glucose homeostasis through enzymatic termination of incretin action. We report that plasma DPP-4 activity correlates with body weight and fat mass, but not glucose control, in mice. Genetic disruption of adipocyte *Dpp4* expression reduced plasma DPP-4 activity in older mice but did not perturb incretin levels or glucose homeostasis. Knockdown of hepatocyte *Dpp4* completely abrogated the obesity-associated increase in plasma DPP-4 activity, reduced liver cytokine expression, and partially attenuated inflammation in adipose tissue without changes in incretin levels or glucose homeostasis. In contrast, circulating levels of soluble DPP4 (sDPP4) were dissociated from inflammation in mice with endothelial-selective or global genetic inactivation of *Dpp4*. Remarkably, inhibition of DPP-4 enzymatic activity upregulated circulating levels of sDPP4 originating from endothelial or hematopoietic cells without inducing systemic or localized inflammation. Collectively, these findings reveal unexpected complexity in regulation of soluble versus enzymatic DPP-4 and control of inflammation and glucose homeostasis.

INTRODUCTION

Type 2 diabetes mellitus (T2D) is a metabolic disorder characterized by hyperglycemia, resulting from a combination of islet cell dysfunction (insufficient insulin and excess glucagon secretion) and insulin resistance. Incretin hormones, principally glucagon-like peptide 1 (GLP-1) and glucose-dependent insulinotropic polypeptide (GIP), contribute to control of islet function. Their bioactivity is regulated by the enzymatic activity of dipeptidyl

peptidase-4 (DPP-4), a widely expressed serine protease (Deacon, 2004; Mulvihill and Drucker, 2014; Omar and Ahren, 2014). Plasma DPP-4 activity increases with obesity, and this increase has been postulated to contribute to reduced incretin activity in the setting of obesity and insulin resistance (Ahmed et al., 2017).

DPP-4 also modulates local and systemic inflammation through cleavage of immunoregulatory DPP-4 substrates (Donath and Shoelson, 2011; Mulvihill and Drucker, 2014; Waumans et al., 2015). Notably, systemic reduction of DPP-4 activity achieved through administration of highly selective DPP-4 inhibitors reduces glycaemia in subjects with T2D (Deacon, 2018; Mulvihill and Drucker, 2014; Sandoval and D'Alessio, 2015; Vella, 2012). DPP-4 inhibitors also reduce inflammation in pre-clinical studies and in human subjects with T2D (Makdissi et al., 2012; Mulvihill and Drucker, 2014; Satoh-Asahara et al., 2013; Zhuge et al., 2016). Nevertheless, the precise cell types and tissues critical for linking DPP-4 activity to the control of (1) glucose homeostasis and (2) inflammation are complex and remain incompletely understood (Mulvihill et al., 2017; Omar and Ahren, 2014).

Several studies have proposed that circulating soluble DPP-4 (sDPP4) is released from adipose tissue and acts as a pro-inflammatory adipokine, linking expansion of adipose tissue with increased inflammation, insulin resistance, and metabolic syndrome (Chowdhury et al., 2016; Lamers et al., 2011; Sell et al., 2013; Zillesen et al., 2016). Indeed, increased plasma DPP-4 activity accompanies adipose tissue expansion in humans, rats, and mice (Kirino et al., 2009; Lamers et al., 2011; Mulvihill et al., 2017; Zhuge et al., 2016). Moreover, small interfering RNA-mediated depletion of *Dpp4* from human primary adipocytes improved adipocyte insulin sensitivity (Rohrborn et al., 2016), whereas treatment with sDPP4 directly activated inflammatory signaling pathways *ex vivo* (Lee et al., 2016; Romacho et al., 2016).

A complementary body of evidence supports a role for hepatic *Dpp4* in the control of metabolism. Liver *DPP4* expression is elevated in subjects with hepatic fat accumulation (Miyazaki et al., 2012), and hepatic *Dpp4* expression correlates with the



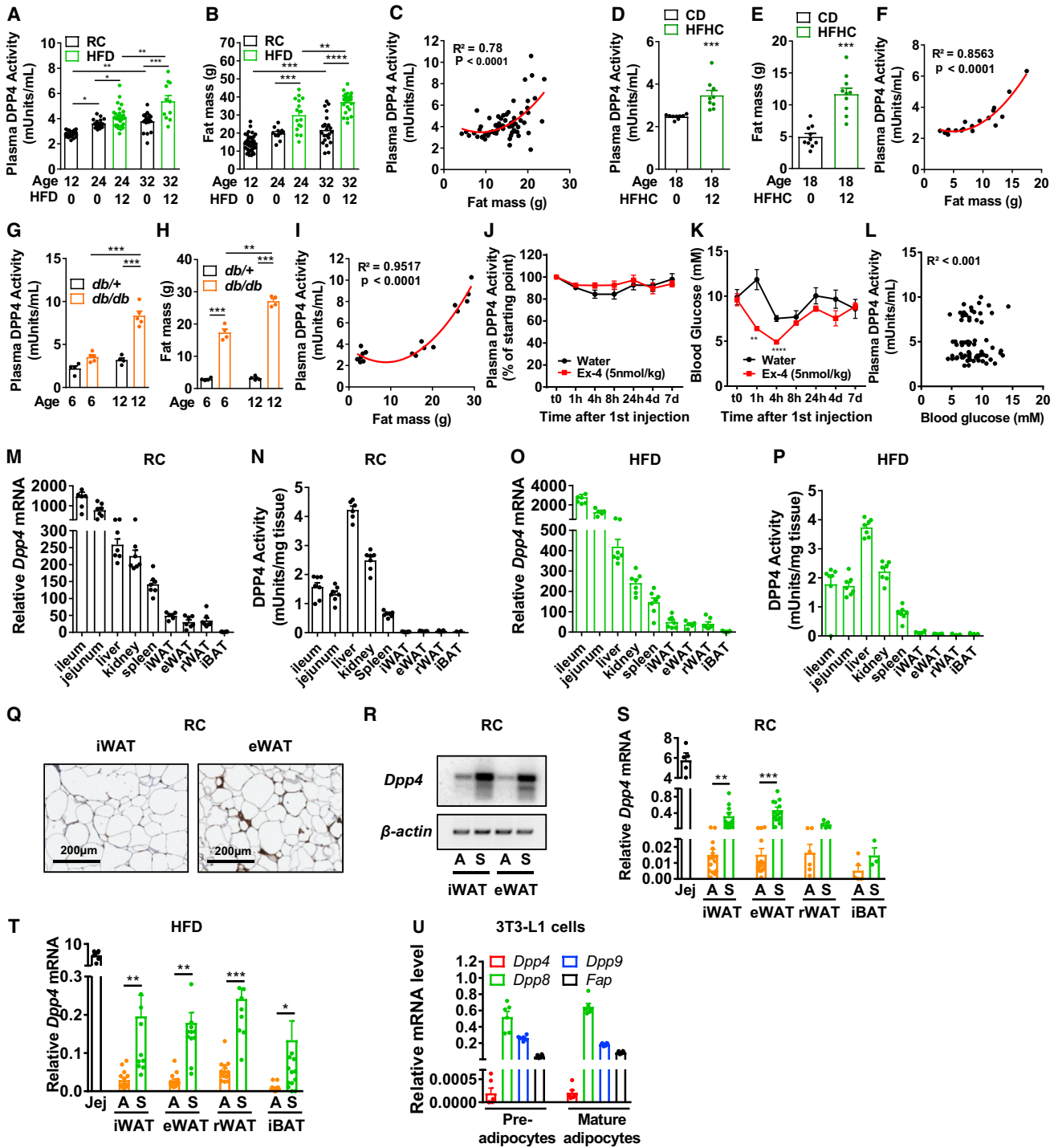


Figure 1. Plasma DPP4 Activity Increases with Age and Obesity

(A–I) Plasma DPP-4 activity in mice fasted for 5 hr (A, D, and G), fat mass as measured by Echo-MRI (B, E, and H), and the correlation between plasma DPP-4 activity and fat mass (C, F, and I) in control mice (8–12 weeks old) fed a regular chow (RC) diet, or after 12 weeks of high-fat diet (HFD) (45% kcal from fat, 24- or 32-week-old mice) (A–C) ($n = 11$ –30/group), or in 18-week-old WT mice fed a control diet (CD) or 40% fat, 20% fructose, 2% cholesterol diet (HFHC) for 12 weeks (D–F) ($n = 9$ /group), or in 6- or 12-week-old *db/+* and *db/db* mice (G–I) ($n = 5$ /group) fed RC.

(J–L) Plasma DPP-4 activity (J), non-fasted blood glucose (K), and the correlation between both (L) in WT mice fed the HFD for 10–20 weeks, and then intra-peritoneally (i.p.) injected twice a day with 5 nmol/kg of Ex-4 (10:00 and 18:00 h) or vehicle for 7 days ($n = 5$ /group).

(M–R) Relative *Dpp4* mRNA level (M and O) and DPP-4 activity (N and P) in the indicated tissues in 24-week-old male mice fed an RC diet (M and N) or fed the HFD for 12 weeks (O and P) ($n = 7$ /group).

(Q) DPP-4 immunostaining in inguinal white adipose tissue (iWAT) and epididymal WAT (eWAT) of 24-week-old WT male mice maintained on an RC diet.

(legend continued on next page)

degree of hepatosteatosis, insulin resistance, and plasma DPP-4 activity (Balaban et al., 2007; Baumeier et al., 2017a). Moreover, transgenic mice overexpressing *Dpp4* in the liver exhibit increased liver and adipose tissue inflammation and insulin resistance (Baumeier et al., 2017b).

Ghorpade et al. (2018) suggested that liver DPP-4 acts as a hepatokine by demonstrating a role for hepatocyte-derived sDPP4 in control of adipose tissue inflammation, insulin resistance, and glucose homeostasis. Accordingly, we have now assessed the metabolic importance of DPP-4 enzymatic activity and circulating levels of DPP4 through generation and analysis of mice with loss of *Dpp4* in multiple tissues and cell types. Adipocyte *Dpp4* was expressed at very low levels and contributed modestly to plasma DPP-4 activity, and selective loss of adipocyte *Dpp4* did not meaningfully impact concentrations of active incretin hormones or glucose homeostasis. In contrast, we find that hepatocyte-derived DPP-4 is the source of obesity-associated increases in plasma DPP-4 activity. However, while hepatocyte-derived DPP-4 controls hepatic and adipose tissue inflammation, it is dispensable for systemic glucose control. Interestingly, the reduction in local inflammation following selective targeting of hepatocyte *Dpp4* is not recapitulated in two different mouse models presenting partial or total reduction in plasma DPP4 activity and circulating sDPP4. Finally, we reveal a feedback loop linking systemic inhibition of DPP-4 enzymatic activity to upregulation of circulating protein levels of DPP4 (sDPP4). These findings reveal dissociation of circulating levels of sDPP4, DPP-4 enzyme activity, and control of obesity-associated inflammatory signals in the liver and adipose tissue.

RESULTS

Plasma DPP-4 Activity Increases with Age and Obesity

Plasma DPP-4 activity increased with age and high-fat diet (HFD) feeding (Figure 1A) and correlated with increased fat mass or increased body weight (Figures 1B, 1C, S1A, and S1B). Plasma DPP-4 activity and fat mass or body weight were also increased and correlated in mice fed a high-fat, high-fructose, high-cholesterol (HFHC) diet (Figures 1D–1F, S1C, and S1D) and in regular chow (RC)-fed *db/db* mice (Figures 1G–1I, S1E, and S1F). In contrast, plasma DPP-4 activity did not correlate with fluctuations in glucose levels in HFD-fed mice treated with or without the GLP-1R agonist exendin-4 (Ex-4, 5 nmol/kg, twice daily) (Figures 1J–1L). Hence plasma DPP-4 activity increases with weight gain and correlates with adipose tissue mass.

DPP-4 Expression and Activity in Adipose Tissue

As increased levels of plasma DPP-4 have been proposed to arise from adipose tissue, reflecting its role as a putative adipo-

kine (Lamers et al., 2011; Sell et al., 2013; Zillessen et al., 2016), we examined the relative tissue expression of *Dpp4* mRNA and DPP-4 activity after RC or HFD feeding for 12 weeks (Figures S1G–S1I). Levels of *Dpp4* mRNA transcripts were much higher in ileum and jejunum compared with levels in white adipose tissue (WAT) depots in RC-fed mice (Figure 1M). In contrast, DPP-4 activity was greater in liver relative to gut tissues and extremely low in WAT depots (Figure 1N). Similar results were detected after 12 weeks of HFD feeding (Figures 1O and 1P); levels of *Dpp4* mRNA (Figure 1O) and DPP-4 activity (Figure 1P) remained 25- to 70-fold lower in WAT depots, relative to levels in gut, liver, and kidney.

Although DPP-4 expression has been extensively characterized in adipocytes (Lamers et al., 2011; Lessard et al., 2015), after isolating adipocytes from stromal vascular fractions (SVFs) (Figures S1J and S1K) we localized DPP-4 protein and *Dpp4* mRNA predominantly to the non-adipocyte cell population within adipose tissue (Figures 1Q and 1R). *Dpp4* mRNA transcripts were more abundant in the SVF from inguinal WAT (iWAT), epididymal WAT (eWAT), retroperitoneal WAT (rWAT), and interscapular brown adipose tissue of RC- and HFD-fed mice (Figures 1R–1T). To determine whether *Dpp4* expression was modulated during adipocyte differentiation, we assessed *Dpp4* mRNA expression throughout differentiation in 3T3-L1 cells (Figures 1U and S1L). *Dpp4* expression was unchanged throughout the 8-day process despite significant increases in well-described markers of differentiation such as lipoprotein lipase (*Lpl*), peroxisome proliferator activated receptor (*Pparγ*), fatty acid binding protein 4 (*Fabp4*), adiponectin (*Adipoq*), and CCAAT/enhancer-binding protein a (*Cebpa*) (Figure S1L); notably, *Dpp4* expression was 200- to 3,000-fold less abundant than three related members of the same enzyme family (*Dpp8*, *Dpp9*, and *Fap*) (Figure 1U).

Genetic Targeting of Adipocyte *Dpp4*

Despite low levels of adipocyte *Dpp4* expression in fat from RC- and HFD-fed mice, we could not rule out a metabolic role for adipocyte DPP-4 under conditions of weight gain and expansion of adipocyte tissue mass. Accordingly, we crossed *Dpp4*^{Flox/Flox} mice (Mulvihill et al., 2017) with mice expressing Cre recombinase under control of the adiponectin promoter to generate *Dpp4*^{Adipo^{-/-}} mice (Lee et al., 2013). Analysis of genomic DNA (gDNA) from *Dpp4*^{Adipo^{-/-}} mice revealed selective recombination of the *Dpp4* gene in DNA from WAT adipocytes (Figures S2A and S2B). Nevertheless, body weight, fat mass, WAT depot, and liver mass were not different (Figures S2C–S2E) and plasma DPP-4 activity and DPP-4 protein concentrations, fasting glucose, glucose tolerance, and plasma levels of insulin and intact GLP-1 were similar in *Dpp4*^{Adipo^{+/+}} versus *Dpp4*^{Adipo^{-/-}} mice on RC and after 20 weeks of HFD feeding

(R) Full-length *Dpp4* and β -actin PCR products amplified from cDNA generated from mature adipocyte (A) and SVF (S) isolated from iWAT or eWAT of 12-week-old WT mice.

(S and T) Relative *Dpp4* expression (versus *Ppia*) in control tissue (Jej, Jejunum) and in mature adipocytes (A) and SVF (S) isolated from iWAT, eWAT, retroperitoneal white adipose tissue (rWAT), and interscapular brown adipose tissue (iBAT) of 12-week-old WT mice fed RC (S) or in 24-week-old mice after 12 weeks of HFD feeding (T) (n = 5–10/group).

(U) Relative *Dpp4*, *Dpp8*, *Dpp9*, and *Fap* expression (versus *Tbp*) in 3T3-L1 cells before induction of differentiation (preadipocytes) and after 8 days of differentiation (mature adipocytes) (n = 6/group).

Data are presented as the means \pm SEM. *p \leq 0.05, **p \leq 0.01, ***p \leq 0.001, ****p \leq 0.0001 using one-way ANOVA (A, B, G, H, S, and T) or t test (D and E). See also Figure S1.

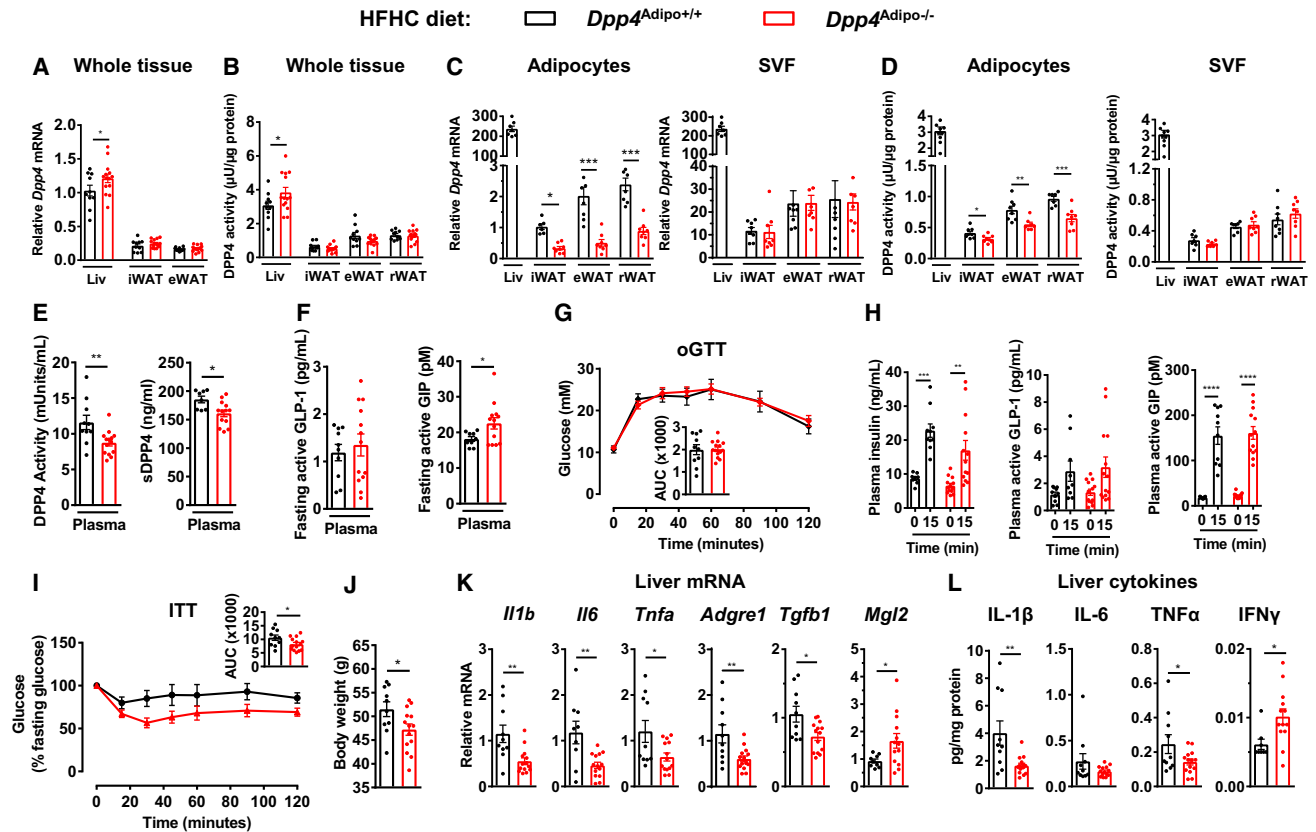


Figure 2. The Contribution of Adipocyte-Derived DPP-4 to Metabolic Phenotypes in Older Mice

(A–D) *Dpp4* mRNA (A and C) (relative to *Ppia*) or DPP4 activity (B and D) in whole tissue (A and B) or in adipocyte or SVF (C and D) isolated from 1-year-old Adiponectin-Cre (black, *Dpp4*^{Adipo+/+}) and *Dpp4*^{Adipo-/-} (red) mice fed an HFHC diet for 4 weeks ($n = 8$ /group).

(E–H) Plasma DPP4 activity and DPP4 protein (here called soluble DPP4, sDPP4) (E), plasma levels of fasting active GLP-1 and active GIP (F), glucose excursion, and area under the curve (AUC) (G), and plasma insulin, active GLP-1, and active GIP before (0) and 15 min after glucose gavage (H) during an oral glucose tolerance test (oGTT) (5 hr fast, 2 g/kg glucose) ($n = 10$ –14/group).

(I and J) Glucose excursion during insulin tolerance test (ITT) (5 hr fast, 0.5 U/kg insulin), and body weight (J) in 1-year-old *Dpp4*^{Adipo+/+} and in *Dpp4*^{Adipo-/-} mice after 2–4 weeks on HFHC diet ($n = 10$ –14/group).

(K and L) Hepatic mRNA abundance (relative to *Tbp*) (K) and liver protein concentrations of inflammatory mediators (L) in 1-year-old *Dpp4*^{Adipo+/+} and *Dpp4*^{Adipo-/-} mice after 4 weeks on HFHC diet ($n = 10$ –14/group).

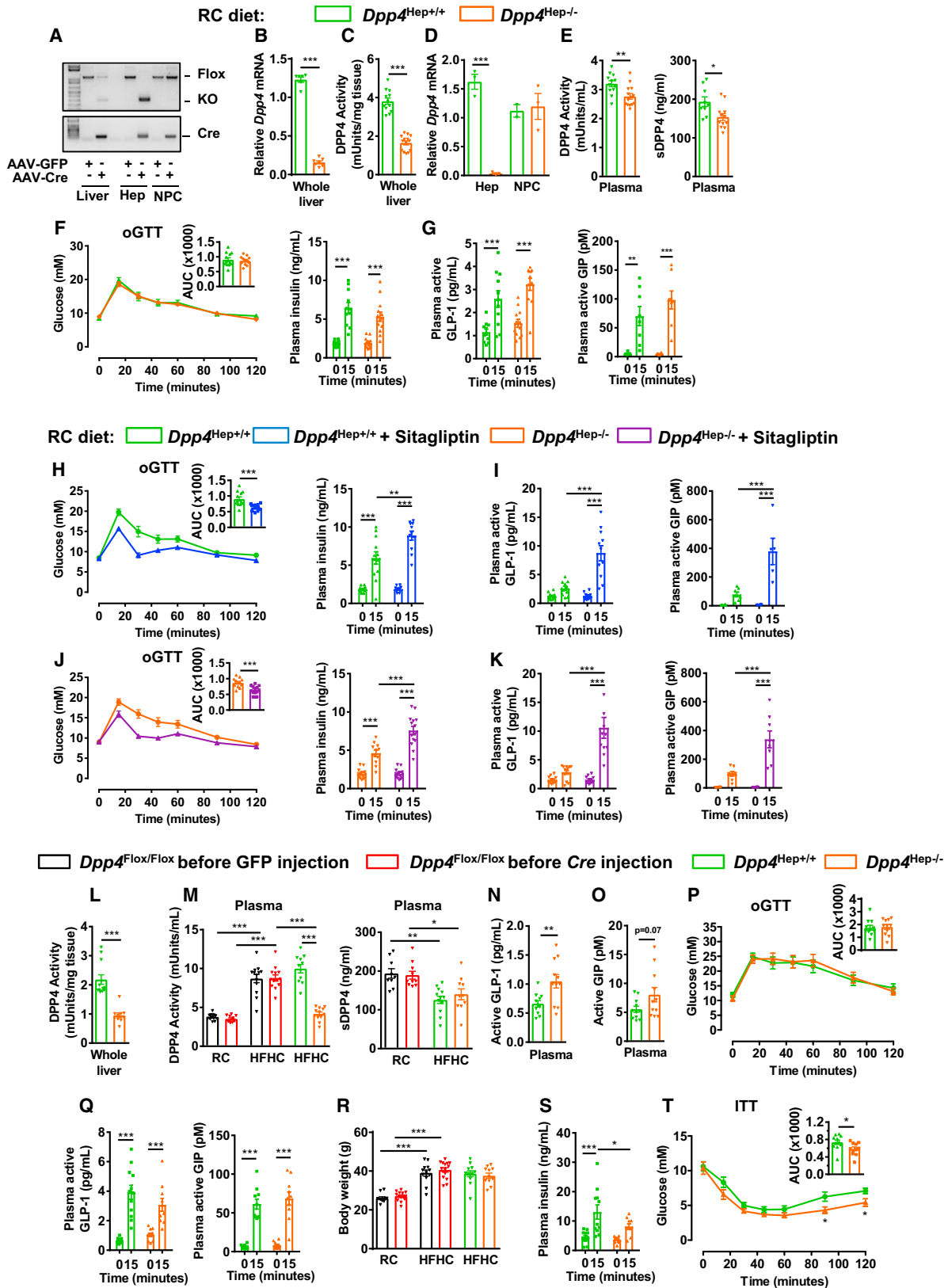
Data are presented as the means \pm SEM. * $p \leq 0.05$, ** $p \leq 0.01$, *** $p \leq 0.001$ using one-way ANOVA (A–D), t test (E–G and I–L), or a two-way ANOVA (H). WAT, white adipose tissue; Liv, liver; iWAT, inguinal WAT; eWAT, epididymal WAT; rWAT, retroperitoneal WAT. See also Figures S2 and S3.

(Figures S2F–S2I). Moreover, the DPP-4 inhibitor sitagliptin improved glucose tolerance and augmented glucose-stimulated levels of insulin and GLP-1 to a similar extent after RC (Figures S2J and S2K) or HFD feeding (Figures S2L and S2M) in *Dpp4*^{Adipo+/+} versus *Dpp4*^{Adipo-/-} mice. Hence, adipocyte-derived DPP-4 is expressed at very low levels, and is not essential for basal or diet-induced obesity-associated increases in plasma DPP-4 activity, incretin degradation, glucose homeostasis, or the glucoregulatory response to sitagliptin in adult mice up to 32 weeks of age.

The Contribution of Adipocyte-Derived DPP-4 to Metabolic Phenotypes in Older Mice

To assess whether adipocyte DPP-4 expression increases with age, we studied 1-year-old *Dpp4*^{Adipo-/-} HFHC-fed mice. *Dpp4* mRNA and DPP-4 activity remained relatively higher in liver versus WAT from older wild-type (WT) and *Dpp4*^{Adipo-/-} mice (Figures 2A and 2B), and levels of *Dpp4* mRNA and DPP-4 activ-

ity were not different in whole adipose tissue depots from older *Dpp4*^{Adipo-/-} versus *Dpp4*^{Adipo+/+} mice (Figures 2A and 2B). Nevertheless, levels of *Dpp4* mRNA and DPP-4 activity were reduced in isolated adipocyte fractions (but not the SVF) from iWAT, eWAT, and rWAT of older *Dpp4*^{Adipo-/-} mice (Figures 2C and 2D). Furthermore, plasma DPP-4 activity and circulating levels of sDPP4 were reduced and levels of active GIP, but not GLP-1, were increased in older *Dpp4*^{Adipo-/-} mice (Figures 2E and 2F). However, oral glucose tolerance, and plasma levels of glucose-stimulated insulin, active GLP-1, and GIP were unchanged (Figures 2G and 2H). Insulin tolerance was improved (Figure 2I), in the context of a slight reduction in body weight (Figure 2J). *Dpp4*^{Adipo-/-} mice also exhibited reduced hepatic levels of mRNA and/or protein for interleukin-1β (IL-1β), IL-6, tumor necrosis factor alpha (TNF-α), F4/80 (*Adgre1*), and transforming growth factor β1, and an increase in interferon-γ (IFN-γ) protein and mRNA levels of the anti-inflammatory M2 macrophage marker *Mgl2* (Figures 2K, 2L, S3A, and S3B). In contrast,



(legend on next page)

levels of cytokine mRNA transcripts and protein concentrations were not different in eWAT and iWAT, except for an increase in CXCL1 in eWAT and plasma (Figures S3C–S3G). Taken together, adipocyte-derived DPP-4 contributes to the pool of circulating sDPP4 and DPP-4 activity in older, obese HFHC-fed mice, yet its elimination is not associated with major impairment in the control of incretin levels or glucose homeostasis.

Hepatocyte DPP-4 Contributes to Plasma DPP-4 Activity, but Not to Glucose Control

As hepatocyte-derived DPP-4 has been proposed to function as a hepatokine (Baumeier et al., 2017b; Ghorpade et al., 2018), we assessed whether endogenous hepatocyte-derived DPP-4 contributes to the circulating pool of DPP-4 activity and control of glucose homeostasis. We used an adeno-associated virus (AAV) expressing Cre recombinase under the control of the thyroxine-binding globulin (TBG) promoter (Sun et al., 2012) to generate *Dpp4*^{Hep^{-/-}} mice. Injection of AAV-TBG-Cre recombined gDNA in liver, selectively in hepatocytes (Figure 3A), and markedly reduced total hepatic *Dpp4* expression and DPP-4 activity (Figures 3B and 3C). A near complete elimination of *Dpp4* expression was detected specifically in hepatocytes (Figure 3D), and not in the non-parenchymal cell fraction (Figures 3D, S4A, and S4B). In contrast, no recombination of the *Dpp4* gene, reduction of *Dpp4* expression, or DPP-4 activity was detected in kidney, spleen, lung, or jejunum in RC-fed *Dpp4*^{Hep^{-/-}} mice (Figures S4D–S4F), or in iWAT or eWAT after RC or HFHC feeding (Figure S4G) in *Dpp4*^{Hep^{-/-}} mice. RC-fed *Dpp4*^{Hep^{-/-}} mice (Figure S4I) exhibited a small reduction in plasma levels of DPP-4 activity and protein (sDPP4) (Figure 3E). However, glucose tolerance and plasma levels of insulin, active GLP-1, and GIP were not different before and after glucose challenge in *Dpp4*^{Hep^{+/+}} mice versus *Dpp4*^{Hep^{-/-}} mice (Figures 3F and 3G). Hepatic and plasma triglycerides and plasma non-esterified fatty acids were not different in *Dpp4*^{Hep^{+/+}} versus *Dpp4*^{Hep^{-/-}} mice (Figures S4K and S4L). Moreover, hepatocyte-derived DPP-4 was not required for the glucoregulatory response to the DPP-4 inhibitor sitagliptin, which improved glucose tolerance and increased plasma levels of insulin, active GLP-1, and active GIP to a similar extent in *Dpp4*^{Hep^{+/+}} versus *Dpp4*^{Hep^{-/-}} mice (Figures 3H–3K).

Increased Plasma DPP-4 Activity in HFHC-Fed Mice Is Derived from Hepatocytes

We next examined the contribution of hepatocyte DPP-4 to plasma DPP-4 activity and glucose homeostasis after HFHC feeding for 10 weeks (Figure S4J), a diet shown to increase circulating DPP-4 activity (Figure 1D) and induce metabolic inflammation in multiple tissues, including the liver (Hsieh et al., 2016). Liver DPP-4 activity was markedly reduced and the increase in plasma DPP-4 activity associated with HFHC feeding was totally abolished in HFHC-fed *Dpp4*^{Hep^{-/-}} mice (Figures 3L and 3M). Nevertheless, circulating levels of sDPP4 in *Dpp4*^{Hep^{-/-}} mice were not different from *Dpp4*^{Hep^{+/+}} mice (Figure 3M). Fasting plasma levels of active GLP-1 were increased and GIP trended higher in fasted *Dpp4*^{Hep^{-/-}} mice (Figures 3N and 3O). However, glucose tolerance and circulating levels of glucose-stimulated intact GLP-1 and GIP were similar in *Dpp4*^{Hep^{-/-}} versus *Dpp4*^{Hep^{+/+}} mice (Figures 3P–3Q). Although body weight was not different (Figure 3R), plasma levels of glucose-stimulated insulin were reduced and insulin sensitivity was modestly increased, reflecting delayed recovery of glycemia, in HFHC-fed *Dpp4*^{Hep^{-/-}} mice (Figures 3S and 3T).

Hepatocyte-Derived DPP-4 Influences Inflammation in the Liver and Adipose Tissue

As the reduction of sDPP4 and DPP-4 activity has been linked to reduced local tissue and systemic inflammation (Ghorpade et al., 2018; Mulvihill and Drucker, 2014), we assessed cytokine mRNA levels and protein concentrations in the liver of RC- and HFHC-fed *Dpp4*^{Hep^{-/-}} mice. Intriguingly, hepatic levels of *Ccl2*, *Adgre1*, *Il2*, and *Acta2* mRNAs were reduced, and *Tnfa* trended lower in HFHC-fed *Dpp4*^{Hep^{-/-}} mice (Figures 4A and S5A). Levels of the M2 anti-inflammatory macrophage markers *Mgl2* and *Arg1* were unchanged (Figure S5A), and the mRNA encoding the DPP-4 binding protein *Ada* was increased (Figure 4A). Moreover, hepatic cytokine protein concentrations of CXCL1, 1L-1 β , IL-2, IL-5, and IL-6 were lower in HFHC-fed *Dpp4*^{Hep^{-/-}} mice (Figures 4B and S5C). Furthermore, mRNA levels of *Adgre1* (F4/80), *Il1b*, *Il2*, *Il12b*, and *Ccl2* were lower, and protein levels of TNF- α and IL-1 β were reduced in eWAT from *Dpp4*^{Hep^{-/-}} mice (Figures 4C, 4D, S5B, and S5D). The increase in *Adgre1* mRNA expression in adipose tissue from HFHC-fed control mice versus *Dpp4*^{Hep^{-/-}} mice corresponded with results of

Figure 3. Hepatocyte-Derived DPP-4 Contributes to Plasma DPP-4 Activity, but Not to Glucose Control

(A–D) Genomic DNA recombination in whole liver, isolated hepatocytes (Hep), or the isolated non-parenchymal cell (NPC) fraction (A), *Dpp4* mRNA expression in whole liver (B) (n = 6–7/group), DPP-4 activity in whole liver (C) (n = 14/group), and *Dpp4* mRNA level in hepatocytes and NPC fractions (D) (n = 3/group) sampled from 12-week-old female *Dpp4*^{Flox/Flox} mice 2 weeks after intravenous injection of AAV-TBG-GFP (green, *Dpp4*^{Hep^{+/+}}) or AAV-TBG-Cre (orange, *Dpp4*^{Hep^{-/-}} mice).

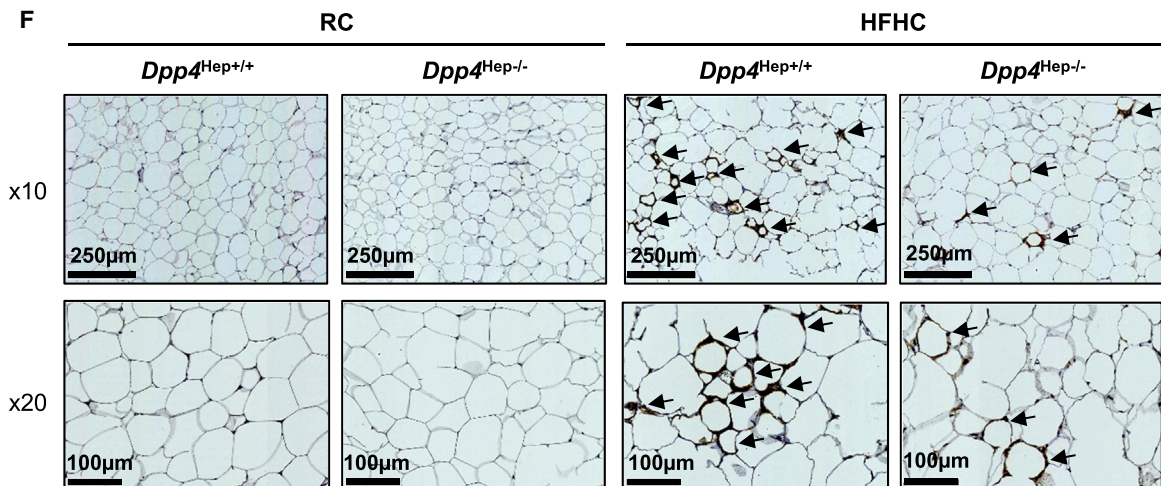
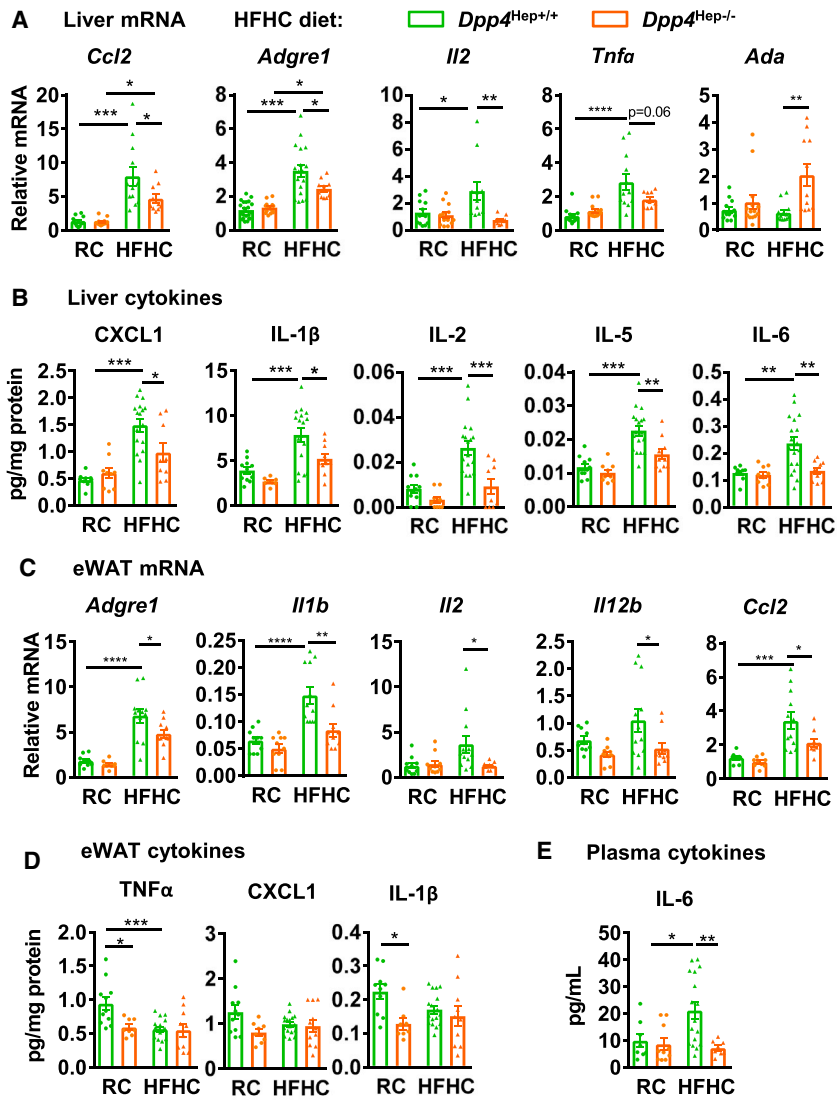
(E) Plasma DPP-4 activity and plasma DPP4 protein concentrations (soluble DPP4, sDPP4) 4 weeks after AAV injection (n = 14/group).

(F and G) Glucose excursion, AUC, plasma insulin (F), and plasma levels of active incretin hormones (G) before and 15 min after glucose gavage during oGTT (5 hr fast, 2 g/kg glucose) in *Dpp4*^{Hep^{+/+}} and *Dpp4*^{Hep^{-/-}} mice fed an RC diet (7–12 days after AAV injection) (n = 13/group).

(H–K) Glucose excursion, AUC, plasma insulin (H and J), and plasma active incretin hormone levels (I and K) before and 15 min after glucose gavage, in response to water (blue) (or acute inhibition of DPP-4 (10 mg/kg sitagliptin, 1 mg/mL solution, given by gavage 30 min before glucose) in *Dpp4*^{Hep^{+/+}} and *Dpp4*^{Hep^{-/-}} mice under RC diet conditions (n = 13/group).

(L–T) Liver DPP-4 activity (L), plasma DPP-4 activity, and plasma DPP4 protein concentrations (sDPP4) in mice fed RC or HFHC diets for 10 weeks prior to AAV injection, and 4 weeks following AAV injection (HFHC + virus) (M), 5-hr-fasted plasma levels of active GLP-1 and active GIP (N and O), glucose excursion and AUC (P) and incretin hormones (Q) during OGTT, body weights before and after 10 and 14 weeks of HFHC diet (R), insulin during OGTT (S), glucose excursion during an insulin tolerance test (1 U/kg insulin) (T) 3 weeks after AAV injection, and in HFHC diet-fed *Dpp4*^{Hep^{+/+}} and *Dpp4*^{Hep^{-/-}} mice (n = 10–12/group).

Data are presented as the means \pm SEM. *p \leq 0.05, **p \leq 0.01, ***p \leq 0.001 using t test (B, C, E, L, N–P, and T), one-way-ANOVA (D, M, and R), or a two-way ANOVA (F–K, Q, and S). See also Figure S4.



(legend on next page)

immunostaining showing a reduction in crown-like structures in eWAT of *Dpp4*^{Hep-/-} mice (Figure 4F). Selective reduction of hepatocyte-derived DPP-4 also reduced levels of plasma IL-6 (Figure 4E), without affecting plasma levels of IL-2, IL-5, IL-10, IFN- γ , IL-1 β , TNF- α , and CXCL1 (Figure S5E).

Reduction of sDPP4 and DPP-4 Activity in *Dpp4*^{EC-/-} Mice Does Not Reduce Markers of Tissue or Systemic Inflammation

As endothelial and hematopoietic cells also contribute to the circulating pool of plasma DPP-4 activity (Mulvihill et al., 2017), we assessed local and systemic inflammation in RC- and HFD-fed *Dpp4*^{EC-/-} mice. Consistent with the reduction of plasma DPP-4 activity (Figure 5A) (Mulvihill et al., 2017), circulating levels of sDPP4 were substantially reduced in *Dpp4*^{EC-/-} mice (Figure 5A). Nevertheless, insulin tolerance was not different under RC conditions and was actually impaired in HFD-fed *Dpp4*^{EC-/-} compared with *Dpp4*^{EC+/+} mice (Figures 5B and 5C). Despite lower circulating levels of sDPP4, multiple markers of inflammation were not different in liver, WAT, or plasma from RC- and HFD-fed *Dpp4*^{EC-/-} mice compared with their littermate controls (Figures 5D and S6A–S6F). Surprisingly, TNF- α was increased in eWAT and plasma from HFD-fed *Dpp4*^{EC-/-} mice (Figures 5E and 5F). With prolonged HFD feeding, plasma DPP-4 activity was no longer reduced; however, circulating levels of sDPP4 remained substantially lower in *Dpp4*^{EC-/-} mice (Figure 5G). Collectively, these findings dissociate reductions in circulating levels of sDPP4 from corresponding changes in tissue and systemic inflammation and plasma DPP-4 activity *in vivo*.

Complete Elimination of DPP-4 Expression Does Not Reduce Cytokine Expression in HFD-Fed Mice

To further examine the importance of circulating sDPP4 for hepatic and WAT inflammation, we studied *Dpp4*^{-/-} mice with whole-body inactivation of the *Dpp4* gene (Marguet et al., 2000; Mulvihill et al., 2017). Plasma DPP-4 activity and circulating sDPP4 were markedly diminished or undetectable, respectively, in younger RC- and HFD-fed *Dpp4*^{-/-} mice (Figure 5H). Insulin sensitivity was improved (Figure 5I), and the expression of a number of cytokines was reduced in liver, eWAT, and plasma from RC-fed *Dpp4*^{-/-} mice (Figures 5J–5L and S6G–S6I). In contrast, despite the complete elimination of circulating sDPP4, insulin sensitivity was not improved, and pro-inflammatory cytokine expression was not reduced in WAT, liver, or plasma from HFD-fed *Dpp4*^{-/-} mice (Figures 5M–5P and S6J–S6L).

Dissociation of Circulating Levels of sDPP4, DPP-4 Activity, and Markers of Inflammation

To further understand the relationship between circulating DPP-4 activity and inflammation, we analyzed markers of tissue

and systemic inflammation in HFHC-fed mice treated with the highly selective DPP-4 inhibitor, MK-0626 (Edmondson et al., 2006; Mulvihill et al., 2016). Consistent with previous findings, plasma and tissue DPP-4 activity was markedly suppressed, and plasma active GLP-1 levels were increased in MK-0626-treated mice (Figures 6A–6D). Unexpectedly, HFHC-fed mice treated with MK-0626 exhibited a marked ~4-fold increase in levels of circulating sDPP4 (Figure 6E). Nevertheless, tissue and plasma cytokine levels were not different in HFHC-fed mice with profound suppression of DPP-4 activity, despite elevated levels of sDPP4 (Figures 6F–6H).

Given the emerging role of sDPP4 as a pro-inflammatory mediator (Ghorpade et al., 2018; Zhong et al., 2013), and the surprising increase in sDPP4 levels in mice with robust suppression of DPP-4 enzyme activity (Figures 6A and 6E), we analyzed circulating sDPP4 levels in several additional groups of mice on different diets, treated with and without structurally distinct DPP-4 inhibitors. Plasma DPP-4 activity was suppressed, whereas circulating levels of sDPP4 were consistently increased several-fold in all cohorts of mice treated with MK-0626 for 2–14 weeks (Figures 6I–6L). Furthermore, systemic DPP-4 inhibition, associated with an increase in ventricle inflammation and fibrosis markers (as described in Mulvihill et al., 2016), was also associated with increased circulating levels of sDPP4 in HFD-fed diabetic mice exposed to sham or transaortic constriction surgery (Figure 6M). Importantly, upregulation of circulating levels of sDPP4 was also observed within several days following administration of two clinically approved DPP-4 inhibitors in the drinking water, sitagliptin and linagliptin (Figures 6N–6O).

To determine the cellular origin of sDPP4 induced by treatment of mice with DPP-4 inhibitors, we analyzed *Dpp4*^{Hep-/-}, *Dpp4*^{Adipo-/-}, *Dpp4*^{Gut-/-} and *Dpp4*^{EC-/-} mice after HFHC feeding and continuous administration of a DPP4i (MK-0626) for 5 weeks. MK-0626 reduced plasma DPP-4 activity in all groups of mice (left panels, Figures 7A–7D). Plasma levels of sDPP4 were increased following MK-0626 administration in *Dpp4*^{Hep-/-}, *Dpp4*^{Adipo-/-}, and *Dpp4*^{Gut-/-} mice (Figures 7A–7C, right panels). In contrast, MK-0626 suppressed DPP-4 enzymatic activity but failed to robustly upregulate levels of circulating sDPP4 in *Dpp4*^{EC-/-} mice (Figure 7D). These findings indicate that DPP-4 inhibition requires *Dpp4* expression in Tie2⁺ cells of hematopoietic or endothelial lineage for maximal upregulation of circulating levels of sDPP4. Collectively, these experiments identify unexpectedly complex relationships between plasma DPP-4 enzyme activity, circulating levels of sDPP4, and the control of inflammation and glucose homeostasis (Figures 7E and S7).

DISCUSSION

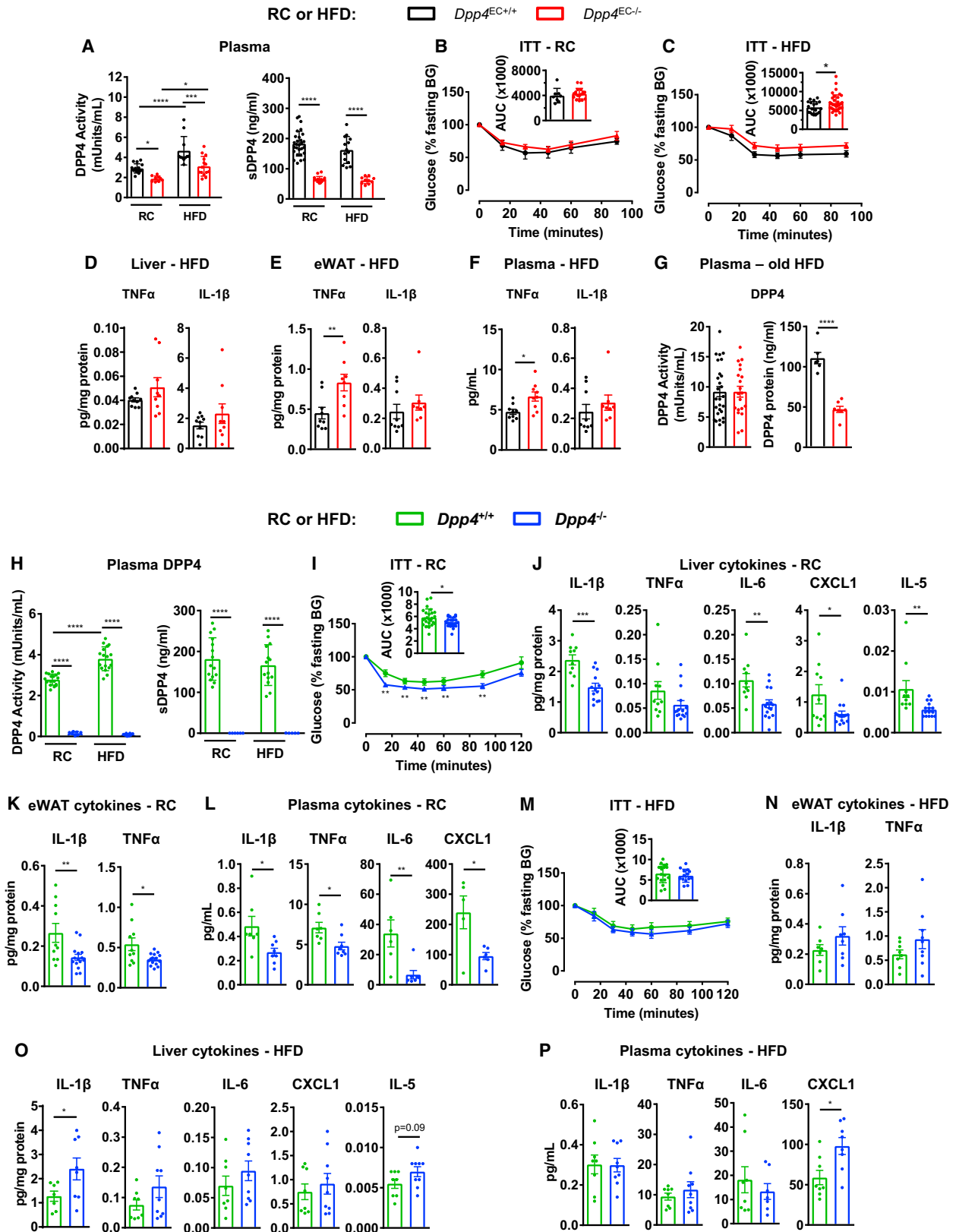
Clinical reports associating increased plasma levels of DPP-4 and circulating DPP-4 activity with weight gain and insulin

Figure 4. Hepatocyte-Derived DPP-4 Controls Inflammation in the Liver and Adipose Tissue

(A–E) mRNA levels (relative to *Tbp*) (A and C) and protein concentrations (B, D, and E) of inflammatory markers in liver (A and B), eWAT (C and D), and plasma (E) 4 weeks after injection of AAV-TGB-GFP or AAV-TGB-Cre in *Dpp4* flox male mice that were fed an RC or HFHC diet for 14 weeks. Data are presented as the means \pm SEM. * $p \leq 0.05$, ** $p \leq 0.01$, *** $p \leq 0.001$, **** $p \leq 0.0001$ using one-way ANOVA.

(F) Representative images (magnification $\times 10$ and $\times 20$) of immunostaining for F4/80 in eWAT of the same mice as in (A–E). Arrows indicate macrophages presenting in crown-like structures.

See also Figure S5.



(legend on next page)

resistance (Mulvihill and Drucker, 2014; Sell et al., 2013) prompted us to determine the source and metabolic relevance of obesity-associated alterations in DPP-4 expression and activity. Despite studies implicating DPP-4 as an adipokine (Lamers et al., 2011; Sell et al., 2013), *Dpp4* expression was relatively low in WAT depots and most abundant within cells of the SVF, as described previously (Shin et al., 2017; Zhong et al., 2013; Zhuge et al., 2016). Moreover, *Dpp4* expression did not increase to a meaningful extent in WAT from HFD-fed mice. Analysis of *Dpp4*^{Adipo^{-/-}} mice up to 32 weeks of age did not reveal reduction in basal or HFD-stimulated plasma DPP-4 activity, or any apparent changes in plasma levels of intact incretin hormones or glucose homeostasis. Furthermore, *Dpp4* expression was not induced during an 8-day differentiation of mouse 3T3-L1 fibroblasts to mature adipocytes. One-year-old HFHC-fed *Dpp4*^{Adipo^{-/-}} mice exhibited a selective reduction in WAT *Dpp4* expression and DPP-4 activity and reduced plasma DPP-4 activity. However, these findings were not accompanied by evidence for compelling alterations in glucose homeostasis. Hence, adipocyte DPP-4 activity is not critical for the control of incretin activity and glucose metabolism in mice.

In contrast, selective genetic reduction of hepatocyte-derived *Dpp4* expression completely attenuated the increase of plasma DPP-4 activity in mice with diet-induced obesity. Intriguingly, loss of hepatocyte DPP-4 led to an increase in fasting levels of active GLP-1, and active GIP trended higher. Nevertheless, this reduction in hepatocyte and plasma DPP-4 activity was not associated with increased levels of intact incretin hormones after glucose administration, nor any improvements in glucose tolerance. These findings are consistent with our recent observations that reduction of DPP-4 in different cellular compartments, such as endothelial cells, hematopoietic cells, and enterocytes, produces differential effects on incretin degradation, plasma DPP-4 activity, and potentiation of the enteroendocrine axis (Mulvihill et al., 2017). Hence, our current findings extend the concept of compartment-specific DPP-4 expression in the control of incretin hormone cleavage by establishing a limited role for hepatocyte DPP-4 in the regulation of bioactive GLP-1 selectively in the fasting state.

A number of intriguing findings were noted in mice with attenuation of hepatocyte *Dpp4* expression. First, levels of several cytokine mRNA transcripts and proteins were lower in the liver and adipose tissue of mice with reduced hepatocyte *Dpp4* expression. Importantly, robust systemic catalytic inhibition of DPP-4 activity (including plasma and liver) of HFHC-fed

mice did not recapitulate the anti-inflammatory phenotype(s) observed in *Dpp4*^{Hep^{-/-}} mice. These findings are consistent with recent studies linking hepatocyte-derived sDPP4, independent of its catalytic activity, to the control of adipocyte inflammation (Dong et al., 1996; Ghorpade et al., 2018; Ishii et al., 2001; Zhong et al., 2013).

Although anti-inflammatory actions have been described following inhibition of DPP-4 activity in multiple cell types and tissues, the literature contains contradictory reports as to whether the anti-inflammatory actions of DPP-4 are dependent on (Lee et al., 2016; Shinjo et al., 2015; Zhuge et al., 2016), or independent (Ghorpade et al., 2018; Zhong et al., 2013) of, its enzymatic catalytic activity. Notably, enhanced expression of hepatic DPP-4 and levels of circulating DPP-4 activity and protein correlate with features of steatohepatitis in preclinical and clinical studies (Baumeier et al., 2017a, 2017b; Williams et al., 2015). Nevertheless, systemic inhibition of DPP-4 catalytic activity with sitagliptin did not attenuate the extent of biopsy-proven steatohepatitis or fibrosis in a randomized control trial in human subjects (Joy et al., 2017). These latter findings are consistent with lack of change in urinary cytokine levels following 1 month of daily sitagliptin administration in humans with T2D (Lovshin et al., 2017).

The demonstration that sDPP4 derived from high-fat-fed mouse hepatocytes augments pro-inflammatory activity in visceral adipose tissue via macrophage caveolin-1 (Ghorpade et al., 2018) prompted us to re-assess the correlation between sDPP4 expression and inflammation. Although tissue and circulating markers of inflammation were reduced in RC-fed *Dpp4*^{-/-} mice, inflammation was not reduced in tissues from HFD-fed *Dpp4*^{-/-} mice despite complete loss of sDPP4. Furthermore, RC- or HFD-fed *Dpp4*^{EC^{-/-}} mice exhibited substantially lower levels of circulating sDPP4, yet no reduction in levels of pro-inflammatory cytokines in the liver, WAT, or the circulation. As high-fat feeding would be expected to induce the secretion of liver-derived sDPP4 and augment WAT macrophage inflammation (Ghorpade et al., 2018), our data using multiple animal models reveal an unanticipated dissociation between absence or reduction of circulating sDPP4, the cellular source of sDPP4, and the extent of systemic and tissue inflammation in different lines of HFD-fed mice.

Even more surprising was the finding that selective DPP-4 inhibition with MK-0626, a clinical backup candidate for sitagliptin (Edmondson et al., 2006; Mulvihill et al., 2016), was associated with marked induction of circulating levels of sDPP4. Notably, we reproduced this observation in multiple different cohorts of

Figure 5. Partial or Total Reduction of DPP-4 Expression and Plasma DPP-4 Activity Does Not Reduce Markers of Tissue or Systemic Inflammation in HFD-Fed Mice

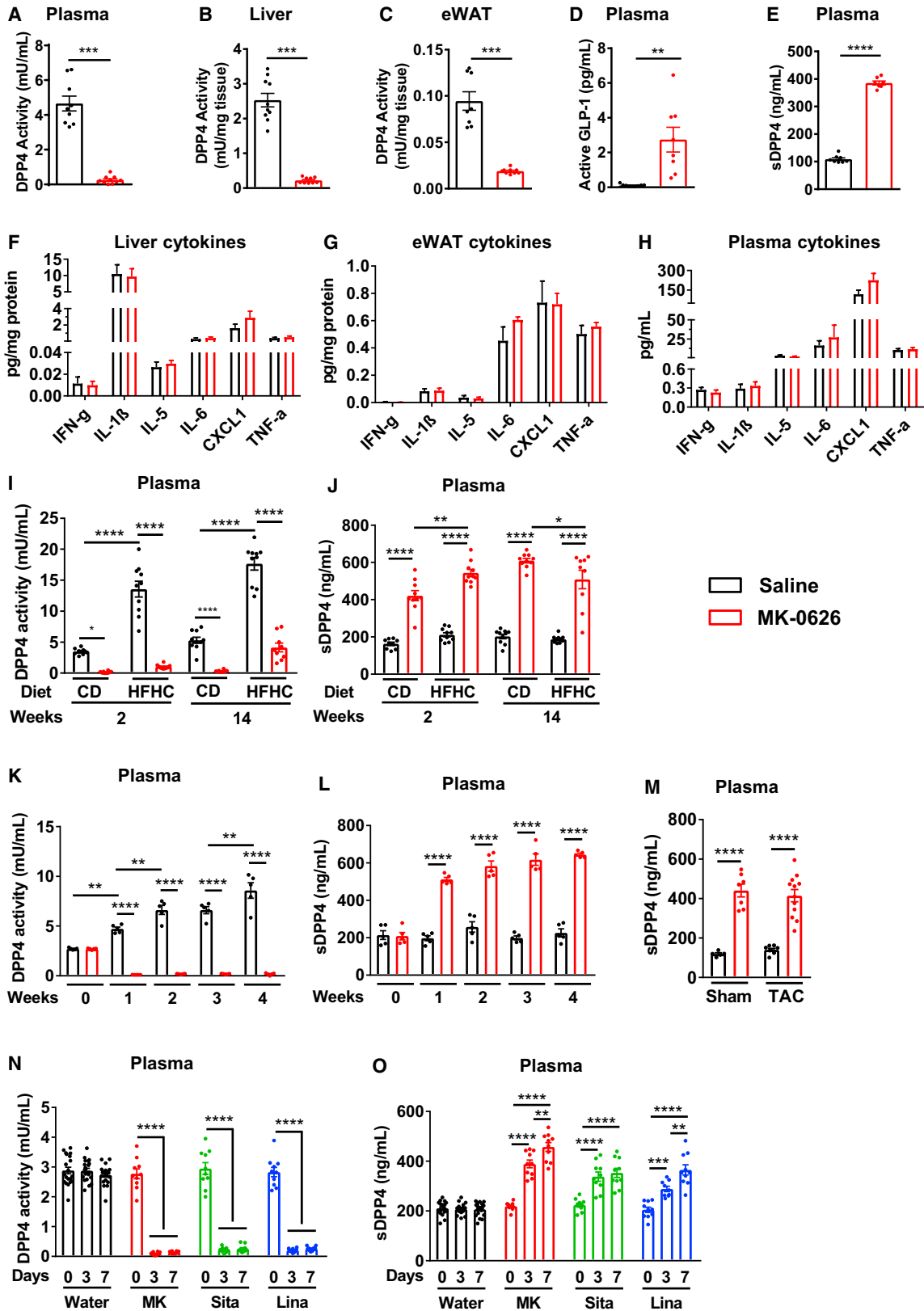
(A–C) Plasma DPP-4 activity and plasma-soluble DPP-4 protein (sDPP4) (A), as well as glucose excursion and AUC during an insulin tolerance test (ITT) (0.5 U/kg insulin in B or 1 U/kg insulin in C) in *Dpp4*^{EC^{+/+}} (Tie2-Cre mice, black) and *Dpp4*^{EC^{-/-}} (red) mice fed an RC diet (8–12 weeks old) (A and B) or after 8 weeks of HFD (16–20 weeks old) (A and C) (n = 9–25/group).

(D–F) Protein concentrations of cytokines in liver (D), eWAT (E) and plasma (F) of 16- to 20-week-old *Dpp4*^{EC^{+/+}} (Tie2-Cre mice) and *Dpp4*^{EC^{-/-}} mice after 8–12 weeks of HFD (n = 9/group).

(G) Plasma DPP-4 activity and plasma-soluble DPP-4 protein (sDPP4) in *Dpp4*^{EC^{+/+}} and *Dpp4*^{EC^{-/-}} mice fed the HFD for 25–30 weeks (n = 20–27/group for activity; n = 6–7/group for protein).

(H–P) Plasma DPP-4 activity and plasma-soluble DPP-4 protein concentrations (sDPP4) (H) (n = 6–14/group), glucose excursion and AUC during ITT (0.5 U/kg insulin in I or 1 U/kg insulin in M) in *Dpp4*^{-/-} (blue) and *Dpp4*^{+/+} (green, WT littermate control mice) mice fed an RC diet (8–12 weeks old) (H and I) or after 8–12 weeks on HFD (H and M) (n = 15–25/group). Protein concentrations of inflammatory markers in liver (J and O), eWAT (K and N) and plasma (L and P) of *Dpp4*^{+/+} and *Dpp4*^{-/-} mice fed RC (16–20 weeks old) (J–L) or after 12–15 weeks of HFD (20–25 weeks old) (N–P) (n = 6–10/group).

Data are presented as the means ± SEM. *p ≤ 0.05, **p ≤ 0.01, ***p ≤ 0.001, ****p ≤ 0.0001 using one-way ANOVA (A and H) or t test (B–G and I–P). See also Figure S6.



(legend on next page)

mice, on different diets, treated for various time periods (2–14 weeks) (Figure 7). Moreover, we demonstrated that treatment of mice with either sitagliptin or linagliptin, two widely used clinically approved DPP-4 inhibitors, also rapidly increased circulating levels of sDPP4. Furthermore, our experiments using mouse genetics demonstrated that *Dpp4* expression within Tie2⁺ hematopoietic or endothelial cells is required for the DPP-4 inhibitor-mediated induction of circulating sDPP4. The putative importance of hematopoietic cells for generation of sDPP4 identified here is also consistent with results of bone marrow transplantation experiments in DPP-4-deficient rats and mice (Casrouge et al., 2018; Wang et al., 2014).

Surprisingly, we were unable to find previous reports describing upregulation of sDPP4 levels in the context of catalytic DPP-4 inhibition in animals or humans. Intriguingly, sitagliptin rapidly and dose-dependently induced expression of the *DPP4* gene in SerpinB3-expressing human liver cell lines *ex vivo* (Fasolato et al., 2018), consistent with the existence of an autoregulatory feedback loop linking reduction of DPP-4 activity to augmentation of DPP-4 production. Indeed, enzymatic inhibition of angiotensin-converting enzyme activity or neutral peptidase activity also induced the expression of the cognate enzymes (Helin et al., 1994), in keeping with a model linking inhibition of enzyme activity with upregulation of enzyme biosynthesis.

Collectively, several reports support a direct pro-inflammatory role for sDPP4 in cell types such as lymphocytes, macrophages, and smooth muscle cells (Ghorpade et al., 2018; Ohnuma et al., 2007; Wronkowitz et al., 2014; Zhong et al., 2013; Zhuge et al., 2016). Nevertheless, our current findings dissociate the circulating levels of endogenous sDPP4 and the extent of systemic and WAT inflammation in multiple different mouse models (Figure S7). Furthermore, the demonstration that selective inhibition of DPP-4 enzymatic activity leads to robust induction of circulating sDPP4 without concomitant changes in inflammation raises further questions about the experimental and pathophysiological context linking changes in levels of sDPP4 to pro-inflammatory pathways. Intriguingly, DPP-4 inhibitors are widely used in conjunction with metformin, an agent associated with (1) reduced levels of circulating sDPP4 (Ahmed et al., 2015; Zhong et al., 2015) and (2) decreased numbers of major cardiovascular events, relative to DPP-4 inhibitors alone, in cardiovascular outcome studies (Crowley et al., 2017). Given the widespread use of DPP-4 inhibitors in human subjects with diabetes and inflammatory co-morbidities, including cardiovascular disease (Mulvihill and Drucker, 2014), it seems prudent to

further elucidate the circumstances and co-factors linking changes in soluble and tissue DPP-4 with ambient DPP-4 activity, and sDPP4-mediated regulation of inflammation.

Limitations of Study

An important limitation of these experiments is the exclusive analysis of mouse models. Hence we are as yet unable to determine whether sDPP4 correlates with inflammation or is upregulated by catalytic DPP-4 inhibition in humans. Furthermore, the majority of our mice were normoglycemic or modestly dysglycemic, analyzed following RC or HFD feeding conditions. Hence, whether the inflammatory activity of sDPP4 varies in animal models with different genetic or acquired forms of diabetes, and insulin resistance, requires further analysis. Finally, we observed robust upregulation of sDPP4 in the context of sustained robust inhibition of DPP-4 enzyme activity. In contrast, humans administered DPP-4 inhibitors for the treatment of diabetes are likely to experience less sustained inhibition of DPP-4 enzyme activity over a 24-hr period. Taken together, our findings highlight the putative translational importance of understanding the link between DPP-4 enzyme inhibition, and the circulating levels of pro-inflammatory sDPP4 in human subjects.

STAR★METHODS

Detailed methods are provided in the online version of this paper and include the following:

- KEY RESOURCES TABLE
- CONTACT FOR REAGENT AND RESOURCE SHARING
- EXPERIMENTAL MODEL AND SUBJECT DETAILS
 - Animals
 - Cell Culture: 3T3-L1 Cells
- METHOD DETAILS
 - Glucose and Insulin Tolerance Tests
 - Experiments with Exendin-4
 - Blood and Tissue Collection
 - Body Weight and Body Composition
 - Mature Adipocytes and SVF Isolation
 - Isolation of Primary Mouse Hepatocyte and Non-parenchymal Cell Fractions
 - Genomic DNA Isolation and Gene Expression
 - Detection of Full Length Mouse *Dpp4* mRNA
 - Immunostaining
- QUANTIFICATION AND STATISTICAL ANALYSIS

Figure 6. Dissociation of Circulating Levels of sDPP4, DPP-4 Activity, and Markers of Inflammation

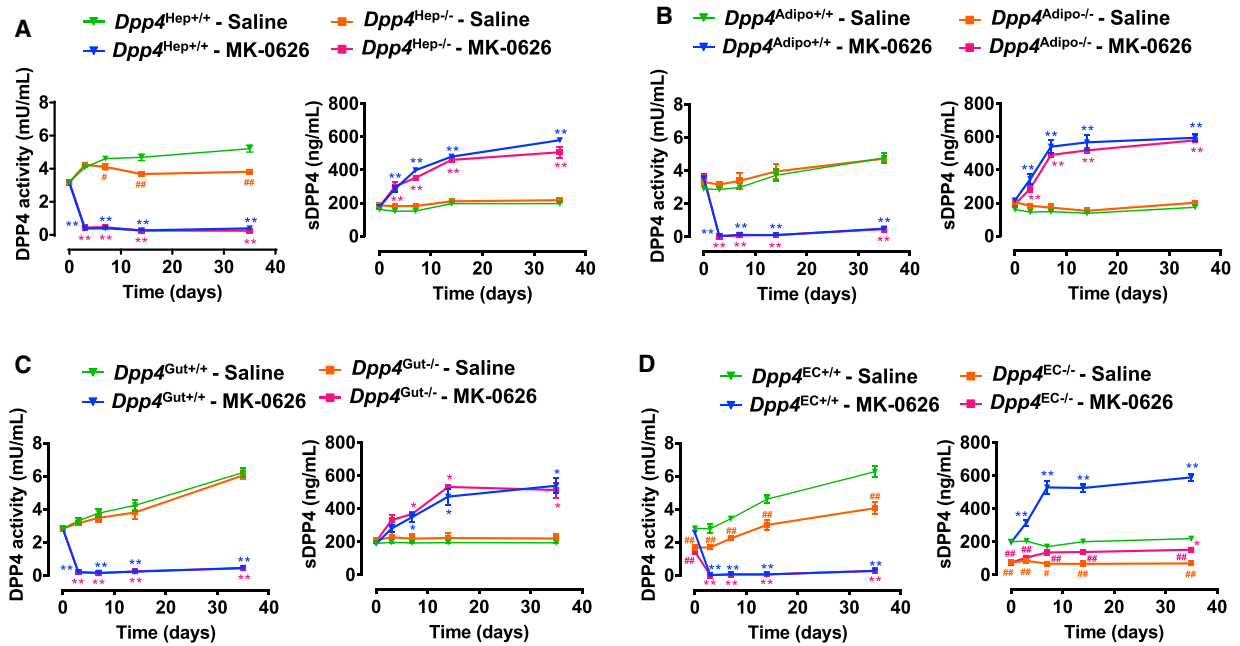
(A–E) DPP-4 activity in plasma (A), liver (B) and eWAT (C), plasma active GLP-1 after a 5-hr fast (D) and plasma-soluble DPP-4 protein concentrations (sDPP4) (E) in control mice (Adiponectin-Cre mice) fed an HFHC diet for 14 weeks (black) or fed an HFHC diet for 10 weeks and then switched to an HFHC diet supplemented with DPP-4 inhibitor (DPP4i) MK-0626 for 4 weeks (red) (n = 7/group).

(F–H) Protein concentrations of inflammatory cytokines in liver (F), eWAT (G), and plasma (H) of control mice fed an HFHC diet for 14 weeks with or without MK-0626 for the last 4 weeks (n = 7/group).

(I–M) Plasma DPP-4 activity (I and K) and plasma-soluble DPP-4 protein concentrations (J, L, and M) in WT mice fed a control diet (CD) or an HFHC diet for 10 weeks, followed by an additional 2 or 14 weeks on HFHC diet ± DPP4i (I and J) (n = 9–10/group), or in 20-week-old WT mice fed an RC diet and then directly switched to either HFHC or HFHC diet + MK-0626 for 1, 2, 3, and 4 weeks (K and L) (n = 5/group), or in WT mice fed HFD for 12 weeks and administered a one-time injection of streptozotocin (90 mg/kg i.p.) and fed HFD + MK-0626 (18 mg/kg food) for an additional 15 weeks and having undergone sham or transaortic constriction (TAC) surgery for initiation of pressure overload-induced heart failure (M) (Mulvihill et al., 2016) (n = 5–12/group).

(N and O) Plasma DPP-4 activity (N) and plasma sDPP-4 protein level (O) in 12-week-old WT mice with free access to water containing either 18 mg/L MK-0626 (MK, red), 4 g/L sitagliptin (Sita, green) or 37.5 mg/L linagliptin (Lina, blue), or no drug (water, black) for 3 or 7 days (n = 10–20/group).

Data are presented as the means ± SEM. *p ≤ 0.05, **p ≤ 0.01, ***p ≤ 0.001, ****p ≤ 0.0001 using t test (A–E) or one-way ANOVA (F–O). See also Figure S7.



E

Genetic Reduction of *Dpp4* Expression and Activity

DPP4 Inhibitors

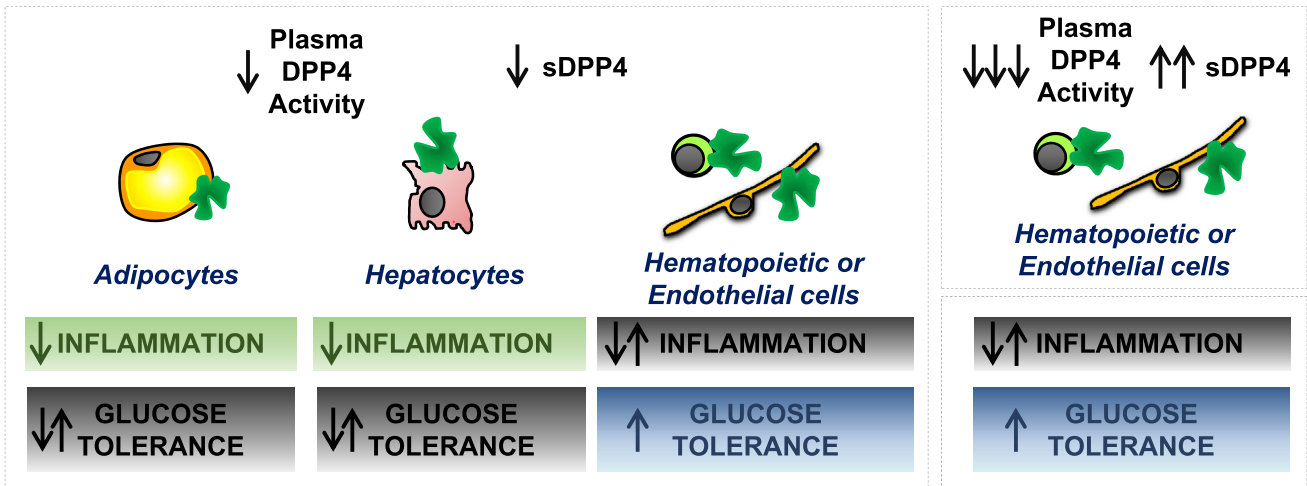


Figure 7. Increase in sDPP4 Induced by DPP-4 Inhibition Originates from Endothelial or Hematopoietic Cells

(A–D) DPP-4 activity (left panels) and circulating DPP-4 protein levels (soluble DPP-4, sDPP4) (right panels) in *Dpp4*^{Hep^{-/-} and their littermate controls (*Dpp4*^{Flox/Flox} injected with AAV-GFP, *Dpp4*^{Hep^{+/+}) (A), *Dpp4*^{Adipo^{-/-} and their littermate controls (Adiponectin-Cre, *Dpp4*^{Adipo^{+/+}) (B), *Dpp4*^{EC^{-/-} and their littermate controls (Tie2-Cre, *Dpp4*^{EC^{+/+}) (C), or in *Dpp4*^{Gut^{-/-} and their littermate controls (Villin-Cre, *Dpp4*^{Gut^{+/+}) (D) fed HFHC diet supplemented or not with MK-0626 (18 mg/kg food) for 0, 3, 7, 14, or 35 days (n = 3–10/group). Data are presented as the means ± SEM. *p ≤ 0.05 and **p ≤ 0.0001 where * indicate the comparisons between the saline- and the MK-treated groups in controls (blue) and in specific knockout (KO) (pink) mice. #p ≤ 0.05 and ##p ≤ 0.0001 where # indicate the comparisons between the controls and the specific KO mice in the saline- (orange) and the MK-treated groups (pink) using one-way ANOVA for each time point. (E) Schematic illustrating the metabolic consequences regarding glucose tolerance and inflammation that ensue following genetic reduction of *Dpp4* expression in adipocytes, hepatocytes, or endothelial and hematopoietic cells versus upregulation of circulating sDPP4 in mice following treatment with a DPP-4 inhibitor.}}}}}}}}

SUPPLEMENTAL INFORMATION

Supplemental Information includes seven figures and can be found with this article online at <https://doi.org/10.1016/j.cmet.2018.10.001>.

ACKNOWLEDGMENTS

The authors would like to acknowledge the Pathology Department at the Center for Modeling Human Disease (CMHD) and the Microscopy Core at the

Lunenfeld-Tanenbaum Research Institute. This work was funded by the IIS (Investigator Initiated Studies Program) no. 56120 from MERK/MSD and by a CIHR Foundation grant to D.J.D. E.M.V. and J.L.B. have received fellowship funding from Diabetes Canada. E.E.M. has received fellowship funding from the Canadian Diabetes Association and the Canadian Institutes of Health Research. G.P. is the recipient of a postdoctoral fellowship from Institut d'Investigacions Biomèdiques August Pi i Sunyer (IDIBAPS). J.E.C. has received fellowships from the Banting and Best Diabetes Centre, University of Toronto, and the Canadian Institutes of Health Research. S. Fazio has received fellowship funding from the LABEX SIGNALIFE (ANR-11-LABX-0028-01 grant). D.J.D. is supported by a Banting and Best Diabetes Centre-Novo Nordisk Chair in Incretin Biology.

AUTHOR CONTRIBUTIONS

Conceptualization, E.M.V., E.E.M., and D.J.D.; Investigation, E.M.V., E.E.M., J.L.B., G.P., S. Fuchs, J.-F.T., S. Fazio, K.K., X.C., L.L.B., D.M., and J.E.C.; Formal Analysis and Visualization, E.M.V. and E.E.M.; Writing – Original Draft, E.E.M., E.M.V., and D.J.D.; Writing – Review & Editing, E.M.V., E.E.M., J.L.B., G.P., S. Fuchs, J.-F.T., S. Fazio, K.K., L.L.B., D.M., J.E.C., and D.J.D.; Funding Acquisition and Project Administration, D.J.D.; Supervision, D.J.D.

DECLARATION OF INTERESTS

D.J.D. has served as a speaker for Eli Lilly and as an advisor or consultant to Kallyope, Merck Research Laboratories, Pfizer, and Novo Nordisk. Mt. Sinai receives investigator-initiated funding from Merck, Novo Nordisk, and Shire for preclinical studies in the Drucker laboratory. E.E.M. has received speaker's honoraria from Merck Canada, and the Ottawa Heart Institute receives funding from Merck for preclinical studies in the Mulvihill laboratory. J.E.C. has received speaker honoraria from Merck. The other authors have no other conflicts of interest relevant to this article to disclose.

Received: February 5, 2018

Revised: May 15, 2018

Accepted: October 5, 2018

Published: November 1, 2018

REFERENCES

Ahmed, R.H., Huri, H.Z., Al-Hamodi, Z., Salem, S.D., and Muniandy, S. (2015). Serum levels of soluble CD26/dipeptidyl peptidase-IV in type 2 diabetes mellitus and its association with metabolic syndrome and therapy with antidiabetic agents in Malaysian subjects. *PLoS One* *10*, e0140618.

Ahmed, R.H., Huri, H.Z., Muniandy, S., Al-Hamodi, Z., Al-Absi, B., Alsalahi, A., and Razif, M.F. (2017). Altered circulating concentrations of active glucagon-like peptide (GLP-1) and dipeptidyl peptidase 4 (DPP4) in obese subjects and their association with insulin resistance. *Clin. Biochem.* *50*, 746–749.

Balaban, Y.H., Korkusuz, P., Simsek, H., Gokcan, H., Gedikoglu, G., Pinar, A., Hascelik, G., Asan, E., Hamaloglu, E., and Tatar, G. (2007). Dipeptidyl peptidase IV (DDP IV) in NASH patients. *Ann. Hepatol.* *6*, 242–250.

Baumeier, C., Saussenthaler, S., Kammel, A., Jahnert, M., Schluter, L., Hesse, D., Canouil, M., Lobbens, S., Caiazzo, R., Raverdy, V., et al. (2017a). Hepatic DPP4 DNA methylation associates with fatty liver. *Diabetes* *66*, 25–35.

Baumeier, C., Schluter, L., Saussenthaler, S., Laeger, T., Rodiger, M., Alaze, S.A., Fritsche, L., Haring, H.U., Stefan, N., Fritsche, A., et al. (2017b). Elevated hepatic DPP4 activity promotes insulin resistance and non-alcoholic fatty liver disease. *Mol. Metab.* *6*, 1254–1263.

Casrouge, A., Sauer, A.V., Barreira da Silva, R., Tejera-Alhambra, M., Sanchez-Ramon, S., IcareB, Cancrini, C., Ingersoll, M.A., Aiuti, A., and Albert, M.L. (2018). Lymphocytes are a major source of circulating soluble dipeptidyl peptidase 4. *Clin. Exp. Immunol.* <https://doi.org/10.1111/cei.13163>.

Chowdhury, H.H., Velebit, J., Radic, N., Francic, V., Kreft, M., and Zorec, R. (2016). Hypoxia alters the expression of dipeptidyl peptidase 4 and induces developmental remodeling of human preadipocytes. *J. Diabetes Res.* *2016*, 7481470.

Crowley, M.J., Williams, J.W., Jr., Kosinski, A.S., D'Alessio, D.A., and Buse, J.B. (2017). Metformin use may moderate the effect of DPP-4 inhibitors on cardiovascular outcomes. *Diabetes Care* *40*, 1787–1789.

Deacon, C.F. (2004). Therapeutic strategies based on glucagon-like peptide 1. *Diabetes* *53*, 2181–2189.

Deacon, C.F. (2018). A review of dipeptidyl peptidase-4 inhibitors. Hot topics from randomized controlled trials. *Diabetes Obes. Metab.* *20 (Suppl 1)*, 34–46.

Donath, M.Y., and Shoelson, S.E. (2011). Type 2 diabetes as an inflammatory disease. *Nat. Rev. Immunol.* *11*, 98–107.

Dong, R.P., Kameoka, J., Hegen, M., Tanaka, T., Xu, Y., Schlossman, S.F., and Morimoto, C. (1996). Characterization of adenosine deaminase binding to human CD26 on T cells and its biologic role in immune response. *J. Immunol.* *156*, 1349–1355.

Edmondson, S.D., Mastracchio, A., Mathvink, R.J., He, J., Harper, B., Park, Y.J., Beconi, M., Di Salvo, J., Eiermann, G.J., He, H., et al. (2006). (2S,3S)-3-Amino-4-(3,3-difluoropyrrolidin-1-yl)-N,N-dimethyl-4-oxo-2-(4-[1,2,4]triazolo [1,5-a]-pyridin-6-ylphenyl)butanamide: a selective alpha-amino amide dipeptidyl peptidase IV inhibitor for the treatment of type 2 diabetes. *J. Med. Chem.* *49*, 3614–3627.

Fasolato, S., Trevelin, E., Ruvoletto, M., Granzotto, M., Zanusi, G., Boscaro, E., Babetto, E., Terrin, L., Battocchio, M.A., Cascato, F., et al. (2018). SerpinB3 induces dipeptidyl-peptidase IV/CD26 expression and its metabolic effects in hepatocellular carcinoma. *Life Sci.* *200*, 134–141.

Flock, G., Baggio, L.L., Longuet, C., and Drucker, D.J. (2007). Incretin receptors for glucagon-like peptide 1 and glucose-dependent insulinotropic polypeptide are essential for the sustained metabolic actions of vildagliptin in mice. *Diabetes* *56*, 3006–3013.

Ghorpade, D.S., Ozcan, L., Zheng, Z., Nicoloso, S.M., Shen, Y., Chen, E., Blüher, M., Czech, M.P., and Tabas, I. (2018). Hepatocyte-secreted DPP4 in obesity promotes adipose inflammation and insulin resistance. *Nature* *555*, 673–677.

Gual, P., Gremeaux, T., Gonzalez, T., Le Marchand-Brustel, Y., and Tanti, J.F. (2003). MAP kinases and mTOR mediate insulin-induced phosphorylation of insulin receptor substrate-1 on serine residues 307, 612 and 632. *Diabetologia* *46*, 1532–1542.

Helin, K., Tikkanen, I., Hohenthal, U., and Fyhrquist, F. (1994). Inhibition of either angiotensin-converting enzyme or neutral endopeptidase induces both enzymes. *Eur. J. Pharmacol.* *264*, 135–141.

Hsieh, J., Koseki, M., Molusky, M.M., Yakushiji, E., Ichi, I., Westertep, M., Iqbal, J., Chan, R.B., Abramowicz, S., Tascu, L., et al. (2016). TTC39B deficiency stabilizes LXR reducing both atherosclerosis and steatohepatitis. *Nature* *535*, 303–307.

Ishii, T., Ohnuma, K., Murakami, A., Takasawa, N., Kobayashi, S., Dang, N.H., Schlossman, S.F., and Morimoto, C. (2001). CD26-mediated signaling for T cell activation occurs in lipid rafts through its association with CD45RO. *Proc. Natl. Acad. Sci. U S A* *98*, 12138–12143.

Joy, T.R., McKenzie, C.A., Tirona, R.G., Summers, K., Seney, S., Chakrabarti, S., Malhotra, N., and Beaton, M.D. (2017). Sitagliptin in patients with non-alcoholic steatohepatitis: a randomized, placebo-controlled trial. *World J. Gastroenterol.* *23*, 141–150.

Kern, M., Klötting, N., Niessen, H.G., Thomas, L., Stiller, D., Mark, M., Klein, T., and Blüher, M. (2012). Linagliptin improves insulin sensitivity and hepatic steatosis in diet-induced obesity. *PLoS One* *7*, e38744.

Kirino, Y., Kamimoto, T., Sato, Y., Kawazoe, K., Minakuchi, K., and Nakahori, Y. (2009). Increased plasma dipeptidyl peptidase IV (DPP IV) activity and decreased DPP IV activity of visceral but not subcutaneous adipose tissue in impaired glucose tolerance rats induced by high-fat or high-sucrose diet. *Biol. Pharm. Bull.* *32*, 463–467.

Kyle, K.A., Willett, T.L., Baggio, L.L., Drucker, D.J., and Grynepas, M.D. (2011). Differential effects of PPAR- γ activation versus chemical or genetic reduction of DPP-4 activity on bone quality in mice. *Endocrinology* *152*, 457–467.

Lamers, D., Famulla, S., Wronkowitz, N., Hartwig, S., Lehr, S., Ouwens, D.M., Eckardt, K., Kaufman, J.M., Ryden, M., Muller, S., et al. (2011). Dipeptidyl

- peptidase 4 is a novel adipokine potentially linking obesity to the metabolic syndrome. *Diabetes* 60, 1917–1925.
- Lee, D.S., Lee, E.S., Alam, M.M., Jang, J.H., Lee, H.S., Oh, H., Kim, Y.C., Manzoor, Z., Koh, Y.S., Kang, D.G., and Lee, D.H. (2016). Soluble DPP-4 up-regulates toll-like receptors and augments inflammatory reactions, which are ameliorated by vildagliptin or mannose-6-phosphate. *Metabolism* 65, 89–101.
- Lee, K.Y., Russell, S.J., Ussar, S., Boucher, J., Vernochet, C., Mori, M.A., Smyth, G., Rourk, M., Cederquist, C., Rosen, E.D., et al. (2013). Lessons on conditional gene targeting in mouse adipose tissue. *Diabetes* 62, 864–874.
- Lessard, J., Pelletier, M., Biertho, L., Biron, S., Marceau, S., Hould, F.S., Lebel, S., Moustarah, F., Lescelleur, O., Marceau, P., and Tchernof, A. (2015). Characterization of differentiating human mature adipocytes from the visceral and subcutaneous fat compartments: fibroblast-activation protein alpha and dipeptidyl peptidase 4 as major components of matrix remodeling. *PLoS One* 10, e0122065.
- Lovshin, J.A., Rajasekeran, H., Lytvyn, Y., Lovblom, L.E., Khan, S., Alemu, R., Locke, A., Lai, V., He, H., Hittle, L., et al. (2017). Dipeptidyl peptidase 4 inhibition stimulates distal tubular natriuresis and increases in circulating SDF-1alpha1-67 in patients with type 2 diabetes. *Diabetes Care* 40, 1073–1081.
- Makdissi, A., Ghanim, H., Vora, M., Green, K., Abuaysheh, S., Chaudhuri, A., Dhindsa, S., and Dandona, P. (2012). Sitagliptin exerts an anti-inflammatory action. *J. Clin. Endocrinol. Metab.* 97, 3333–3341.
- Marguet, D., Baggio, L., Kobayashi, T., Bernard, A.M., Pierres, M., Nielsen, P.F., Ribet, U., Watanabe, T., Drucker, D.J., and Wagtmann, N. (2000). Enhanced insulin secretion and improved glucose tolerance in mice lacking CD26. *Proc. Natl. Acad. Sci. U S A* 97, 6874–6879.
- Miyazaki, M., Kato, M., Tanaka, K., Tanaka, M., Kohjima, M., Nakamura, K., Enjogi, M., Nakamura, M., Kotoh, K., and Takayanagi, R. (2012). Increased hepatic expression of dipeptidyl peptidase-4 in non-alcoholic fatty liver disease and its association with insulin resistance and glucose metabolism. *Mol. Med. Rep.* 5, 729–733.
- Mulvihill, E.E., and Drucker, D.J. (2014). Pharmacology, physiology and mechanisms of action of dipeptidyl peptidase-4 inhibitors. *Endocr. Rev.* 6, 992–1019.
- Mulvihill, E.E., Varin, E.M., Gladanac, B., Campbell, J.E., Ussher, J.R., Baggio, L.L., Yusta, B., Ayala, J., Burmeister, M., Matthews, D., et al. (2017). Cellular sites and mechanisms linking reduction of dipeptidyl peptidase-4 activity to control of incretin hormone action and glucose homeostasis. *Cell Metab.* 25, 152–165.
- Mulvihill, E.E., Varin, E.M., Ussher, J.R., Campbell, J.E., Bang, K.W., Abdullah, T., Baggio, L.L., and Drucker, D.J. (2016). Inhibition of dipeptidyl peptidase-4 impairs ventricular function and promotes cardiac fibrosis in high fat-fed diabetic mice. *Diabetes* 65, 742–754.
- Ohnuma, K., Uchiyama, M., Yamochi, T., Nishibashi, K., Hosono, O., Takahashi, N., Kina, S., Tanaka, H., Lin, X., Dang, N.H., and Morimoto, C. (2007). Caveolin-1 triggers T-cell activation via CD26 in association with CARMA1. *J. Biol. Chem.* 282, 10117–10131.
- Omar, B., and Ahren, B. (2014). Pleiotropic mechanisms for the glucose-lowering action of DPP-4 inhibitors. *Diabetes* 63, 2196–2202.
- Rohrborn, D., Bruckner, J., Sell, H., and Eckel, J. (2016). Reduced DPP4 activity improves insulin signaling in primary human adipocytes. *Biochem. Biophys. Res. Commun.* 471, 348–354.
- Romacho, T., Vallejo, S., Villalobos, L.A., Wronkowitz, N., Indrakusuma, I., Sell, H., Eckel, J., Sanchez-Ferrer, C.F., and Peiro, C. (2016). Soluble dipeptidyl peptidase-4 induces microvascular endothelial dysfunction through proteinase-activated receptor-2 and thromboxane A2 release. *J. Hypertens.* 34, 869–876.
- Sandoval, D.A., and D'Alessio, D.A. (2015). Physiology of proglucagon peptides: role of glucagon and GLP-1 in health and disease. *Physiol. Rev.* 95, 513–548.
- Sato-Asahara, N., Sasaki, Y., Wada, H., Tochiya, M., Iguchi, A., Nakagawachi, R., Odori, S., Kono, S., Hasegawa, K., and Shimatsu, A. (2013). A dipeptidyl peptidase-4 inhibitor, sitagliptin, exerts anti-inflammatory effects in type 2 diabetic patients. *Metabolism* 62, 347–351.
- Sauve, M., Ban, K., Momen, A., Zhou, Y.-Q., Henkelman, R.M., Husain, M., and Drucker, D.J. (2010). Genetic deletion or pharmacological inhibition of dipeptidyl peptidase-4 improves cardiovascular outcomes following myocardial infarction in mice. *Diabetes* 59, 1063–1073.
- Sell, H., Bluher, M., Kloting, N., Schlich, R., Willems, M., Ruppe, F., Knoefel, W.T., Dietrich, A., Fielding, B.A., Arner, P., et al. (2013). Adipose dipeptidyl peptidase-4 and obesity: correlation with insulin resistance and depot-specific release from adipose tissue in vivo and in vitro. *Diabetes Care* 36, 4083–4090.
- Shin, J., Fukuhara, A., Onodera, T., Yokoyama, C., Otsuki, M., and Shimomura, I. (2017). Regulation of dipeptidyl peptidase-4, its substrate chemokines, and their receptors in adipose tissue of ob/ob mice. *Horm. Metab. Res.* 49, 380–387.
- Shinjo, T., Nakatsu, Y., Iwashita, M., Sano, T., Sakoda, H., Ishihara, H., Kushiya, A., Fujishiro, M., Fukushima, T., Tsuchiya, Y., et al. (2015). DPP-IV inhibitor anagliptin exerts anti-inflammatory effects on macrophages, adipocytes, and mouse livers by suppressing NF-kappaB activation. *Am. J. Physiol. Endocrinol. Metab.* 309, E214–E223.
- Sun, Z., Miller, R.A., Patel, R.T., Chen, J., Dhir, R., Wang, H., Zhang, D., Graham, M.J., Unterman, T.G., Shulman, G.I., et al. (2012). Hepatic Hdac3 promotes gluconeogenesis by repressing lipid synthesis and sequestration. *Nat. Med.* 18, 934–942.
- Vella, A. (2012). Mechanism of action of DPP-4 inhibitors – new insights. *J. Clin. Endocrinol. Metab.* 97, 2626–2628.
- Wang, Z., Grigo, C., Steinbeck, J., von Horsten, S., Amann, K., and Daniel, C. (2014). Soluble DPP4 originates in part from bone marrow cells and not from the kidney. *Peptides* 57, 109–117.
- Waumans, Y., Baerts, L., Kehoe, K., Lambeir, A.M., and De Meester, I. (2015). The dipeptidyl peptidase family, prolyl oligopeptidase, and prolyl carboxypeptidase in the immune system and inflammatory disease, including atherosclerosis. *Front. Immunol.* 6, 387.
- Williams, K.H., Vieira De Ribeiro, A.J., Prakoso, E., Veillard, A.S., Shackel, N.A., Brooks, B., Bu, Y., Cavanagh, E., Raleigh, J., McLennan, S.V., et al. (2015). Circulating dipeptidyl peptidase-4 activity correlates with measures of hepatocyte apoptosis and fibrosis in non-alcoholic fatty liver disease in type 2 diabetes mellitus and obesity: a dual cohort cross-sectional study. *J. Diabetes* 7, 809–819.
- Wronkowitz, N., Gorgens, S.W., Romacho, T., Villalobos, L.A., Sanchez-Ferrer, C.F., Peiro, C., Sell, H., and Eckel, J. (2014). Soluble DPP4 induces inflammation and proliferation of human smooth muscle cells via protease-activated receptor 2. *Biochim. Biophys. Acta* 1842, 1613–1621.
- Zhong, J., Gong, Q., Goud, A., Srinivasamaharaj, S., and Rajagopalan, S. (2015). Recent advances in dipeptidyl-peptidase-4 inhibition therapy: lessons from the bench and clinical trials. *J. Diabetes Res.* 2015, 606031.
- Zhong, J., Rao, X., Deulius, J., Braunstein, Z., Narula, V., Hazey, J., Mikami, D., Needleman, B., Satoskar, A.R., and Rajagopalan, S. (2013). A potential role for dendritic cell/macrophage-expressing DPP4 in obesity-induced visceral inflammation. *Diabetes* 62, 149–157.
- Zhuge, F., Ni, Y., Nagashimada, M., Nagata, N., Xu, L., Mukaida, N., Kaneko, S., and Ota, T. (2016). DPP-4 inhibition by linagliptin attenuates obesity-related inflammation and insulin resistance by regulating M1/M2 macrophage polarization. *Diabetes* 65, 2966–2979.
- Zillesen, P., Celner, J., Kretschmann, A., Pfeifer, A., Racke, K., and Mayer, P. (2016). Metabolic role of dipeptidyl peptidase 4 (DPP4) in primary human (pre) adipocytes. *Sci. Rep.* 6, 23074.

STAR★METHODS

KEY RESOURCES TABLE

REAGENT or RESOURCE	SOURCE	IDENTIFIER
Antibodies		
Dipeptidyl peptidase 4 Antibody	R&D Biosystem	Cat# AF954; RRID: AB_355739
F4/80	Abcam	Cat# ab16911; RRID: AB_443548
Bacterial and Virus Strains		
AAV8.TBG.pi.egfp.wpre.bgh	Penn Vector Core	CS0894
AAV8.TBG.PI.CRE.rBG	Penn Vector Core	CS1129
Chemicals, Peptides, and Recombinant Proteins		
Insulin (Humulin) (for ITT)	Eli Lilly and Co.	Cat#VL7510
Insulin, human recombinant, zinc solution (for 3T3-L1)	Thermo Fisher Scientific	12585014
H-Gly-Pro-AMC HBr	Bachem	Cat#I-1225
AMC	Bachem	Cat#Q-1025
Sitagliptin (acute treatment by gavage)	Merck Laboratories	N/A
Sitagliptin (Januvia 100mg) (chronic treatment in drinking water)	Merck Laboratories	N/A
Linagliptin (Trajenta 5mg) (chronic treatment in drinking water)	Eli Lilly	N/A
Exendin-4	Chi Scientific	Custom synthesis
Dulbecco's modified Eagle's medium (DMEM)	Fisher Scientific	41965062
Hepatocyte Wash media	Invitrogen-Gibco	17704024
Liver Perfusion Media	Invitrogen-Gibco	17701038
Liver Digest Media	Invitrogen-Gibco	17703034
Hepatocyte attachment media (Williams E media supplemented with 2 mmol/l glutMAX, 5% fetal bovine serum, 100 U/ml penicillin, 100 µg/ml streptomycin)	Invitrogen-Gibco	A1217601
Fetal calf serum	Life Technologies	10500-064
Isobutylmethylxanthine	Sigma	I5879
Dexamethasone	Sigma	D4902
Rosiglitazone	Enzo Life Science	ALX-350-125-M100
Collagenase Type IA	Sigma	C9891-1G
MK-0626 ((2S,3S)-1-(3,3-difluoropyrrolidin-1-yl)-4-(dimethylamino)-1,4-dioxo-3-(4-[1,2,4]triazolo[1,5-A]pyridin-6-ylphenyl)butan-2-aminium chloride)	Merck Laboratories	N/A
Critical Commercial Assays		
Ultrasensitive Mouse Insulin ELISA	ALPCO	80-INSMSU-E01
Active GLP-1	Mesoscale	150JVC-1
Active GIP	Crystal Chem	81511
Mouse Proinflammatory Panel assay kit	Mesoscale	MSD V-PLEX K15048
Mouse DPPIV/CD26 DuoSet ELISA	R&D System	DY954
Experimental Models: Cell Lines		
3T3-L1 fibroblasts	ATCC	ATCC CL-173
Experimental Models: Organisms/Strains		
<i>Dpp4</i> ^{-/-} mice	Generously provided by Didier Marguet	N/A
<i>Dpp4</i> ^{flox/flox} mice	Merck Laboratories	N/A
B6;FVB-Tg(Adipoq-cre)1Evd/J mice (Adiponectin-cre) mice	Jackson Laboratories	Cat No: 028020
B6.Cg-Tg(Tek-cre)1Ywa/J mice (Tie2-cre) mice	Jackson Laboratories	Cat No: 008863
B6.SJL-Tg(Vil-cre)997Gum/J (Villin-cre) mice	Jackson Laboratories	Cat No: 004586

(Continued on next page)

Continued

REAGENT or RESOURCE	SOURCE	IDENTIFIER
C57BL/6J WT mice	In-house colony at the Toronto Centre for Phenogenomics	N/A
<i>db/db</i> mice	Jackson Laboratories	Cat No: 000697
Oligonucleotides		
actin, alpha 2, smooth muscle, aorta (<i>Acta2a</i>)	Applied Biosystems	Mm01546133_m1
adenosine deaminase (<i>Ada</i>)	Applied Biosystems	Mm00545720_m1
adhesion G protein-coupled receptor E1	Applied Biosystems	Mm00802529_m1
adiponectin	Applied Biosystems	Mm00456425_m1
albumin	Applied Biosystems	Mm00802090_m1
arginase, liver (<i>Arg1</i>)	Applied Biosystems	Mm00475988_m1
CCAAT/enhancer binding protein (C/EBP), alpha	Applied Biosystems	Mm00514283_s1
chemokine (C-C motif) ligand 2	Applied Biosystems	Mm00441242_m1
cyclophilin (<i>ppia</i>)	Applied Biosystems	Mm02342430_g1
delta-like 1 homolog	Applied Biosystems	Mm00494477_m1
dipeptidyl peptidase-4	Applied Biosystems	Mm00494548_m1
fatty acid binding protein 4	Applied Biosystems	Mm00445878_m1
integrin alpha X	Applied Biosystems	Mm00498698
interferon gamma (<i>Iifng</i>)	Applied Biosystems	Mm01168134_m1
interleukin 1 beta	Applied Biosystems	Mm01336189_m1
interleukin 10	Applied Biosystems	Mm99999062_m1
interleukin 2	Applied Biosystems	Mm00434257_m1
interleukin 5	Applied Biosystems	Mm00439645_m1
interleukin 6	Applied Biosystems	Mm00446190_m1
lipoprotein lipase	Applied Biosystems	Mm00434770_m1
macrophage galactose N-acetyl-galactosamine specific lectin 2 (<i>Mgl2</i>)	Applied Biosystems	Mm00460844_m1
peroxisome proliferator activated receptor gamma	Applied Biosystems	Mm01184322_m1
platelet/endothelial cell adhesion molecule 1	Applied Biosystems	Mm01242584_m1
spi-C transcription factor	Applied Biosystems	Mm00488428_m1
transforming growth factor, beta 1 (<i>Tgfb1</i>)	Applied Biosystems	Mm01178820_m1
tumor necrosis factor (<i>tnfa</i>)	Applied Biosystems	Mm00443258_m1
vascular cell adhesion molecule 1	Applied Biosystems	Mm01320970
TATA sequence binding protein (<i>Tbp</i>)	Applied Biosystems	Mm00446973_m1
Software and Algorithms		
Quantity One imaging software	BioRad	http://www.bio-rad.com
Graph Pad Prism 7	Graphpad Software	https://www.graphpad.com
NDP View 2.7.25	Hamamatsu	https://www.hamamatsu.com
Other		
Regular Chow Diet (RC)	Harlan Teklad	Cat No: 2018
High Fat Diet (HFD)	Research Diets	Cat No: D12451
Control diet for HF HC (CD)	Research Diets	Cat No: D09100304
High Fat/High Cholesterol (HFHC) 40% kcal Fat, 20% kcal Fructose, 2% wt./wt. Cholesterol	Research Diets	Cat No: D09100301

CONTACT FOR REAGENT AND RESOURCE SHARING

Further information and requests for resources and reagents should be directed to and will be fulfilled by the Lead Contact, Daniel J. Drucker (drucker@lunenfeld.ca).

EXPERIMENTAL MODEL AND SUBJECT DETAILS

Animals

All experiments were approved by the Animal Care and Use Subcommittee at the Toronto Centre for Phenogenomics, Mt. Sinai Hospital. Room temperature is maintained at 20–22°C. Mice were housed under a 12-h light/dark cycle in the Toronto Centre for Phenogenomics and maintained on regular chow (RC; 18% kcal from fat, 2018, Harlan Teklad, Mississauga, ON or High Fat Diet (HFD; 45% kcal fat, 35% kcal carbohydrate, 0.05% wt./wt. cholesterol, D12451, Research Diets). To induce inflammation, mice were fed a High Fat/High Fructose/High Cholesterol (HFHC) diet (40% kcal Fat, 20% kcal Fructose, 2% wt./wt. Cholesterol, D09100301, Research Diets) and compared with control diet (CD; 10% kcal from fat, D09100304, Research Diets). All mice were given free access to food and water, unless otherwise noted.

Whole body *Dpp4*^{-/-} mice were from a colony described previously (Marguet et al., 2000; Sauve et al., 2010). *db/db* and *db/+* mice were purchased from Jackson laboratories (#000697). Flox *Dpp4*^{Flox/Flox} mice were obtained from Merck Research Laboratories as previously described (Mulvihill et al., 2017). B6;FVB-Tg(Adipoq-cre)1Evdrr/J mice (Adipoq-Cre, Cat # 010803) and B6.Cg-Tg(Tek-cre)1Ywa/J mice (Tie2-Cre, Cat # 008863) were obtained from Jackson Laboratories (Bar Harbor ME). Germline deletion was prevented by restricting *Cre* expression to male breeders. To control for gene dosage, breeders were heterozygous for the *Cre* gene. Intercrossing *Cre*-positive and *Cre*-negative *Dpp4 loxP* heterozygotes from these 2 lines resulted in 6 genotypes: wildtype mice with no *Cre* (WT), mice homozygous for the *LoxP Dpp4* gene (*Dpp4*^{Flox/Flox}), wildtype mice expressing *Cre* recombinase (Adipoq-Cre or Tie2-Cre) and *Dpp4*^{Flox/Flox} mice expressing *Cre* recombinase (*Dpp4*^{Adipo-/-} and *Dpp4*^{EC-/-}). Whenever possible, we carried out experiments in all groups of mice. However, due to lack of phenotypic differences in the control lines (Mulvihill et al., 2017), data are presented as a single control group of pooled Adipoq-Cre and *Dpp4*^{Flox/Flox} mice. All mice were born at the expected Mendelian ratios and appeared healthy. All experiments used age- and sex-matched littermates. For metabolic tests in adult mice, RC diet experiments were performed in 8–12 week old mice, and HFD experiments, in 16–20 week old mice fed the 45% HFD for 8–12 weeks. For experiments in old *Dpp4*^{Adipo-/-} mice, 1-year-old Adipoq-cre and *Dpp4*^{Adipo-/-} mice were put on HFHC and oGTT and ITT were performed after 2 and 3 weeks of HFHC feeding, respectively. Mice were sacrificed and adipocyte and SVF fractions were isolated after 4 weeks on the diet to measure inflammation and assess DPP4 gene knockdown.

To generate *Dpp4*^{Hep-/-} mice, *Dpp4*^{Flox/Flox} adult mice were *i.v.* injected with 1.5×10^{11} GC per mouse (in 100 μ l) of AAV8.TBG.pi.egfp.wpre.bgh (AAV-GFP; control virus) or AAV8.TBG.PI.CRE.rBG (AAV-Cre; a Thyroxin Binding globulin promoter driving *cre* expression that specifically targets hepatocytes, and not Kupffer cells or endothelial cells). Both AAV constructs were obtained from the University of Pennsylvania Vector Core Lab. Most of the experiments were also performed in mice injected with PBS, and as no difference was observed between the GFP and the PBS group, GFP alone was used as a control. For RC diet experiments, female and male mice were injected when 8–12 weeks old. For HFHC experiments, mice were put on diet for 10 weeks, starting when they were 8–12 weeks old, and then injected with virus. Metabolic analyses were performed 1, 2 and 3 weeks after injection and mice were sacrificed 4 weeks post injection.

Chronic inhibition of DPP-4 enzymatic activity was achieved by administering MK-0626 (((2S,3S)-1-(3,3-difluoropyrrolidin-1-yl)-4-(dimethylamino)-1,4-dioxo-3-(4-[1,2,4]triazolo[1,5-A]pyridin-6-ylphenyl)butan-2-aminium chloride) (Edmondson et al., 2006) in the diet (3 mg/kg body weight Merck Laboratories, Rahway, NJ) (Mulvihill et al., 2016). MK-0626 was administered to control mice (Adipoq-cre mice) fed a HFHC diet for 10 weeks. Mice underwent blood collection and oral glucose tolerance testing 2 weeks later and were sacrificed 4 weeks after the start of MK-0626 treatment.

Plasma DPP-4 activity and sDPP4 protein levels in response to DPP4 inhibition, was assessed in 5 independent experiments: 1) WT mice fed CD or HFHC diet for 10 weeks, followed by an additional 2- or 14-weeks on the same diet \pm MK-0626 (18mg/kg food); 2) 20 week-old WT mice fed RC diet and then switched to either HFHC or HFHC + MK-0626 (18mg/kg food) diet for 1, 2, 3 and 4 weeks; 3) 1-year-old STZ-treated (90mg/kg), dysglycemic WT mice fed a HFD \pm MK-0626 (18mg/kg food) and following sham or Transaortic Constriction (TAC) surgery (as described in Mulvihill et al., 2016); 4) MK-0626 (18mg/L water; 2–2.5mg/Kg BW/day); or sitagliptin (4g/L dissolved water; 120–140mg/kg BW/day for the first 24h, then 350–400mg/kg BW/day) or linagliptin (37.5mg/L dissolved in water; 5–5.5mg/kg BW/day) added into the drinking water of 8–12 week-old WT mice for 3 or 7 days. Doses of DPP4 inhibitors were based on previous published studies and pilot studies in our laboratory (Mulvihill et al., 2016, MK-0626; Kyle et al., 2011, Sitagliptin; Kern et al., 2012, Linagliptin). Water bottles were added 24h before the day of the experiment to acclimate the mice. Fresh drug was added every 72 hours. Mice were bled before, as well as 3 and 7 days after starting the treatment. 5) Before or after 3, 7, 14 and 35 days of treatment with MK-0626 (18mg/kg food in HFHC diet) in a) *Dpp4*^{Hep-/-} and *Dpp4*^{Hep+/+} controls (AAV-GFP injected), b) *Dpp4*^{EC-/-} and *Tie2-cre* controls, c) *Dpp4*^{Adipo-/-} and *Adiponectin-cre* controls, and d) *Dpp4*^{Gut-/-} and *Villin-cre* controls (as described in Mulvihill et al., 2016).

The data presented in this research article were from experiments performed in male mice. However, the main experiments supporting our conclusions (plasma DPP4 activity in all mouse models, body weight, insulin and oral Glucose Tolerance Tests, incretin and insulin levels in *Dpp4*^{Hep-/-} vs. their respective controls) were performed in both males and females and the results showed no influence of gender on any of those parameters.

Cell Culture: 3T3-L1 Cells

3T3-L1 fibroblasts were grown at 7% CO₂ and 37C in 35 mm dishes in DMEM, 25 mM glucose, 10% calf serum, and induced to differentiate to adipocytes as previously described (Gual et al., 2003). Briefly, 2 days after reaching confluence, the media was

changed to DMEM, 25 mM glucose, 10% fetal calf serum (FCS), supplemented with isobutylmethylxanthine (0.25 mM), dexamethasone (0.25 μ M), insulin (5 μ g/ml), and pioglitazone (10 μ M). The media was removed after 2 days and replaced with DMEM, 25 mM glucose, 10% FCS, supplemented with insulin (5 μ g/ml) and pioglitazone (10 μ M) for 2 days. The cells were then fed every 2 days with DMEM, 25 mM glucose, 10% FCS. 3T3-L1 cells were harvested at D0, D2, D4, D6, D8 and D10 post-induction into 1 ml Trizol for RNA isolation. Dulbecco's modified Eagle's medium (DMEM), fetal calf serum, and calf serum were obtained from Life Technologies (St Louis, MO, USA). Insulin was from Lilly (Paris, France). All other chemical reagents were purchased from Sigma (St Louis, MO, USA).

METHOD DETAILS

Glucose and Insulin Tolerance Tests

After a 5 hour fast, mice were orally administered water or sitagliptin (Merck Laboratories) at 10 mg/kg (systemic inhibition); followed 30 minutes later by a gavage of 2 g/kg glucose in PBS. For insulin tolerance tests (ITT), human insulin (Humalog, Lilly) was injected (*i.p.*) at a dose of 0.5 U/kg or 1U/kg. Blood for glucose measurements (Contour glucometer, Bayer Healthcare, Toronto, Canada) was obtained from the tail vein before and at 15, 30, 45, 60, 90 and 120 min post-glucose gavage.

Experiments with Exendin-4

Wildtype mice were put on HFD for 10 to 20 weeks (5 in each group), and then *i.p.* injected twice a day with 5 nmol/kg of exendin-4 (10am and 6pm) for 7 days. Blood glucose was recorded and mice were bled at the indicated times for measurement of plasma DPP-4 activity.

Blood and Tissue Collection

All blood samples were collected in heparin-coated capillary microvette tubes and plasma isolated after centrifugation (13,000rpm 5min 4°C). During oral glucose tolerance tests, blood was taken via the tail vein before gavage and 15 min after glucose gavage. For terminal studies, mice were sacrificed by CO₂ inhalation and blood was obtained by cardiac puncture.

For measurement of plasma active GLP-1 (Mesoscale), active GIP (Crystal Chem), and insulin (ultrasensitive insulin ELISA, Alpco Diagnostics), blood was mixed with 10% TED (vol/vol) (5,000 KIU/ml Trasylol, 1.2 mg/ml EDTA and 0.1 nmol/l Diprotin A) and plasma stored at -80°C until further analysis.

To measure the protein levels of pro-inflammatory cytokines and DPP-4 activity, 40-70 mg of liver tissue or 200-350 mg of WAT tissue were homogenized in 500 μ l of lysis buffer (50 mM Tris HCl (pH 8 at 4°C), 1 mM EDTA, 10% glycerol (wt/vol), 0.02% Brij-35 (wt/vol)). Lysis buffer was supplemented with 1 mM dithiothreitol and protease inhibitor for cytokine assay only. Tissue and plasma (containing 10% TED) levels of cytokines were measured using the MSD V-PLEX Mouse Proinflammatory Panel assay kit (Mesoscale). Cytokine concentrations in tissue were normalized to total protein amount measured by Bradford Assay. DPP-4 activity was assessed using a fluorometric assay (substrate: 10 mM H-Gly-Pro-AMC HBr (Bachem #I-1225), standard: AMC (Bachem #Q-1025)) using 10 μ l of plasma (no TED) or 25 μ l of tissue or cell homogenate. DPP-4 activity was normalized to total tissue weight or protein amount. DPP4 protein level was measured using 100 μ l of plasma (diluted 1/120) from 5-hour fasted mice using the mouse DPP4/CD26 DuoSet ELISA kit (DY954; R&D System) following the manufacturer's instructions. Throughout the manuscript, the term "soluble DPP4" (sDPP4) is used to describe the protein level of DPP4 measured in the circulation (plasma).

Body Weight and Body Composition

Body weight was measured once a week after a 5 hour fast. Body composition was measured by EchoMRI quantitative nuclear magnetic resonance (NMR) system (Echo Medical Systems, Houston, TX).

Mature Adipocytes and SVF Isolation

Adipose tissue depots (inguinal, epididymal, retroperitoneal white adipose tissue (WAT) and interscapular brown adipose tissue (BAT)) were isolated from RC-, HFD-, or HFHC diet-fed C56BL/6J mice from the Toronto Centre for Phenogenomics in house colony. Tissues were finely minced on ice, and then digested for 30-50 min in 1mg/ml collagenase in HBSS containing 3% BSA and 5U/ml DNase I at 37°C with gentle agitation. Digestion was stopped with PBS containing 10% FBS and the solution was filtered (500 μ m). Mature adipocytes and SVF fractions were then separated and washed by several successive low speed centrifugations (1000-2000 rpm). The lipid-containing adipocytes floated to the top, whereas the pellet contained the SVF fraction. After washing, cells were either suspended in 1-2 ml Trizol for RNA isolation (and then stored at -80°C) or in homogenization buffer (50 mM Tris HCl (pH 8 at 4°C), 1 mM EDTA, 10% glycerol (wt/vol), 0.02% Brij-35 (wt/vol)) to measure DPP4 activity. For assessment of DPP-4 enzymatic activity, cells were washed twice with PBS to eliminate traces of BSA/FBS. Protein levels were measured by Bradford protein assay. DPP-4 activity was normalized to total protein amount.

Isolation of Primary Mouse Hepatocyte and Non-parenchymal Cell Fractions

Primary hepatocyte isolation was performed on mice anesthetized with Avertin as described (Flock *et al.*, 2007). For purification of the NPC fraction, the hepatocytes were depleted by 2 minutes centrifugation at 50G, and the supernatant containing NPC cells was isolated and centrifuged for 5 minutes at 300G. The pellet was re-suspended in hepatocyte wash medium (Invitrogen-Gibco). Following

4 cycles of hepatocyte depletion, the NPC pellet was enriched in macrophages and endothelial cell markers and depleted of albumin-expressing hepatocytes (Figure S4C) and was collected for further analysis.

Genomic DNA Isolation and Gene Expression

Genomic DNA was isolated from mouse tissue using 50mM NaOH, heating for 10 min at 95°C and then adding a 10% volume of 1M Tris pH8. Total RNA was extracted from tissues using Tri Reagent (Molecular Research Center, Cincinnati, OH). cDNA was synthesized from DNase I-treated (Thermo Fisher Scientific, Markham, ON) total RNA (0.5–3µg) using random hexamers and Superscript III (Thermo Fisher Scientific, Markham, ON). Real-time PCR was carried out using a QuantStudio System and TaqMan Gene Expression Assays (Thermo Fisher Scientific, Markham, ON).

Primer probe sets were manufactured by Taqman Assays-on-Demand (Applied Biosystems). The standard curve method was used to determine mRNA concentrations, and each gene was normalized to cyclophilin (*Ppia*) or TATA box binding protein (*Tbp*) expression, unless otherwise noted.

Detection of Full Length Mouse *Dpp4* mRNA

Total RNA was isolated using TRIzol reagent (Sigma). 2 µg total RNA was reversed transcribed at 50°C for 60 min using Superscript III reverse transcriptase and random hexamers (Sigma). The mouse *Dpp4* gene was amplified by PCR using primer pairs 5'- CAT CAT CAC CGT GCC AAT AG -3' and 5'- TAT CAT CTG CCG TTC CAT GA -3'. Amplification of mouse *Dpp4* cDNA resulted in generation of an approximately 1 kb PCR product. After gel electrophoresis and transfer to nylon membranes, blots were hybridized with a ³²P-labeled mouse (5'- CCA CAC AAA TGT GAA GTC CC -3') *Dpp4* oligonucleotide probe overnight. After washing, blots were visualized using a Storm 860 Phosphor Screen and analyzed with Quantity One imaging software (Bio-Rad).

Immunostaining

Immunostaining was performed by the Pathology core at The Centre for Phenogenomics. Briefly, sections were de-paraffinised and rehydrated. Sections were incubated in methanol + 0.3% H₂O₂ to block endogenous peroxidase activity. Antigen retrieval in TBS containing Proteinase K was performed. Dako protein block was used to block non-specific background staining. Primary antibodies were DPP-4 (R&D Biosytem, AF954) or Mouse F4/80 (Abcam, Cat # ab16911). A biotinylated Rabbit secondary antibody was applied (Vector labs, Cat # BA-4001) followed by Vectastain Elite ABC-HRP peroxidase (Vector laboratories, Cat # PK-6100). Positive staining was visualized using DAB/Plus substrate (Abcam, Cat # ab103723) following manufacturer's instructions. Sections were counter-stained with Mayer's Hematoxylin (Sigma-Aldrich, Cat # MHS32-1L). Digital images were obtained using an Olympus VS120 slide scanner and images were exported using NDP View 2.7.25 software.

QUANTIFICATION AND STATISTICAL ANALYSIS

Results are expressed as the mean ± SEM. Statistical comparisons were made by ANOVA followed by a Tukey post-hoc, a 2-way ANOVA followed by a Sidak post-hoc, or by Student t-test (when only 2 conditions) using GraphPad Prism 7. No methods were used to determine whether the data met assumptions of the statistical approach. Statistical parameters can be found in the figure legends. Statistically significant differences are indicated as * $P \leq 0.05$, ** $P \leq 0.01$, *** $P \leq 0.001$, and **** $P \leq 0.0001$.